3

A Review of Approaches for Measuring Soil Hydraulic Properties and Assessing the Impacts of Spatial Dependence on the Results

Vincenzo Comegna[1], Antonio Coppola[1],
Angelo Basile[2] and Alessandro Comegna[1]
[1]*Dept. For Agricultural and Forestry Systems Management, Hydraulics Division, University of Basilicata, Potenza*
[2]*Institute for Mediterranean Agro-Foresty, (ISAFOM), National Research Centre, Ercolano*
Italy

1. Introduction

The movement of water in the soil and associated solute transport perform a role of primary importance in many applications in the field of hydrology and agriculture. In the sound management of irrigation water, in relation to specific environmental conditions and cropping systems, knowledge of local water flow conditions in zones affected by the root systems is indispensable. Once the irrigation method has been established, only knowledge of the laws governing water flow allows the necessary irrigation frequencies and rates to be established to optimise the distribution of soil moisture, reducing within established limits the effects of water stress and containing water wastage.

Only by studying water dynamics in soil can the contribution of groundwater to water consumption be quantitatively determined. Moreover, the water volumes infiltrating into the soil due to rainfall are strictly linked and governed by the laws of water flow in the soil. No evaluation of water quantities being added to groundwater circulation can be made without first determining the water volumes moving in the zone between the soil surface and the aquifer.

Knowledge of water fluxes, velocities and contents is also indispensable to study the flow of solutes and pollutants and to predict all exchanges, whether chemical or microbiological, occurring in the soil. Within environmental protection initiatives, great weight is attributed to the continuous contribution of solutes characterising any agricultural activity, especially if intensive. Nor should we underestimate the hazards of non-agricultural solute fluxes, and the need to dispose of wastewater, muds and industrial effluent.

Except for situations of direct hazardousness, in general soil and groundwater degradation is linked to the different mobility that solutes may show in the various soil zones. Particular conditions may lead to accumulation zones for certain substances, while in other zones solutes may be easily transported in depth, with consequent alteration of local aquifer

characteristics. To evaluate the nature of the risk represented the presence of these solutes it is important to define the processes governing their movement downward from the soil surface through the vadose zone as far as the aquifer. Only if we know such transport processes can optimal management plans be developed for environmental control with a view to preventing degradation phenomena.

The complexity of such flow processes has encouraged the widespread use of mathematical models corresponding as closely as possible to real phenomena which can supply quantitative evaluations also in the presence of highly complex systems, such as soil-plant-atmosphere continuum (SPAC). To be applied, such models, based on the laws of water flow in the vadose zone, require the relationships linking the volumetric water content, θ, the water potential *h* and the hydraulic conductivity, K.

Moreover, for field applications, an evaluation in statistical terms of the variability of θ-*h*-K relationships is also necessary.

Numerous researches have proposed testing techniques for laboratory and field soil characterization which, however, are almost always laborious and time-consuming (Klute, 1986; Hillel et al., 1998).

The choice of which methodology to adopt for these determinations depends in each case on the particular soil-type and on the local soil conditions. For this reason, it is preferable to have a preliminary soil profile pedological analysis revealing the existence of a distinct horizontal structure or of layers in the soil profile is of particular importance when large areas have to be characterized in terms of transport behavior (Bouma 1983; Coppola et al., 2011).

The purpose of this chapter is to present some experimental procedures for determining the unsaturated hydraulic properties both in the laboratory and open field. It was also developed in view to estimate the structure of the spatial variability exhibited by the available hydrological data set.

2. Soil water flow theory

Soil complexity and the presence of often interacting phenomena make it difficult to study particular aspects of specific processes that always have to be viewed in terms of overall system evolution. Thus in the sector of soil hydrology increasingly sophisticated mathematical models based on real phenomena are being applied. With the support of increasingly available numerical calculators, in many cases such models allow quantitative evaluations to be attained also in the presence of complex systems which are difficult to study (Jury et al., 1991).

In general, such models are based on laws governing water flow and all the physical and chemical processes affecting water transport. These laws have been widely confirmed by experiments and are often reported also in papers in disciplines collateral to soil hydrology (Bear, 1979; Jensen, 1980). Water flow is studied with reference to a porous medium which, on a macroscopic scale, may be considered continuous and in which the various quantities and physical properties are considered functions of position and time. Reference is generally made to isothermal flow processes, to a Newtonian liquid phase and interconnected gaseous phase with a pressure equal to that of the atmosphere. Moreover, due to relatively low

resistance to air flow, the movement of the gaseous phase is neglected and only water flow is referred to.

Such a schematization leads to concrete results when based on a generalized Darcy's law which in the case of isotropic porous media is expressed as follows:

$$v = -K \nabla H \tag{1}$$

in which v is the filtration velocity, K the hydraulic conductivity of the porous medium, ∇ is the Laplacian operator and $H = z + h$ the hydraulic potential of the flow domain, where z is the gravitational head and h the pressure head.

Unlike what happens in filtration processes through saturated porous media, the presence of interconnected air in the pores reduces the effective section of water flow, increasing path tortuosity, which is why conductivity K is variable with water content in volume θ. As regards the pressure head h, it should be pointed out that in unsaturated zones it assumes negative values (matric head), hence the widespread custom in the soil physics literature of referring to it as *suction* or *tension*. Further, as shown by laboratory and field experiments, the link between θ and h is not unique, but is characterised by a multi-value hysteretic function (Mualem and Dagan, 1975).

To study water flow, Darcy's law is coupled to the continuity equation which may be expressed as:

$$\frac{\partial(\rho\theta)}{\partial t} = -\nabla\ (\rho\, v) \tag{2}$$

in which ρ, as is customary, is used to indicate water density and t the time.

Allowing for Darcy's law we obtain from (2):

$$\frac{\partial(\rho\theta)}{\partial t} = \nabla\ (\rho\, K \nabla H) \tag{3}$$

The low water compressibility means that the variation of ρ can be neglected, hence (3) can be written as (Richards' equation):

$$C\frac{\partial h}{\partial t} = \nabla\ \left[K \nabla\ (h + z)\right] \tag{4}$$

in which $C = d\theta/dh$ is the differential water capacity of the porous medium. Or, introducing the diffusion coefficient $D = Kdh/d\theta$, from (3) we obtain the Fokker-Plank equation:

$$\frac{\partial\theta}{\partial t} = \nabla\ (K \nabla z + D \nabla \theta) \tag{5}$$

Having established the initial conditions and those at the boundary of the flow domain, we can then integrate 4 or 5 only if we know at all points the functions $K(\theta)$ and $\theta(h)$ that completely characterise the porous medium in hydraulic terms. Moreover, due to the non-linearity of differential equations 4 and 5 and the fact that functions $K(\theta)$ and $\theta(h)$ (see

Appendix A) cannot always be given a satisfying analytical expression make it necessary adopt numerical integration techniques.

3. Methods of measuring soil hydraulic parameters

The widespread use of increasingly advanced numerical calculators gives us in practice unlimited possibilities of solving differential equations 4 and 5. However, so far there have been limited applications of these solutions to problems of practical interest despite the fact that in many situations there is a considerable need to achieve optimal management, with consequent savings, of irrigation water, as well as a need for soil conservation and groundwater resource protection.

The reasons for this slow spread of soil water flow theory may be sought in the difficult and burdensome task of soil hydraulic characterisation. In particular, hydraulic conductivity $K(\theta)$ is determined with laborious time-consuming methods, it undergoes high variations even with slight changes in water content and in many cases depends on the composition and concentration of circulating solution in the soil (Frenkel et al., 1978). Moreover, the functions $K(\theta)$ and $\theta(h)$, especially at higher water contents, differ according to whether there is a wetting or drainage phase. The choice of methodologies to use for measuring hydraulic characteristics depends on the particular soil and conditions at the measuring point, which is why it is preferable that surveys are preceded by a pedological study. Especially in the case of clayey soils, a critical analysis is required concerning the applicability of the measurement method, the type of probes to be used and the dimensions of the soil volume to which measurements refer.

Hydraulic characteristics may be determined using field or laboratory experiments, operating on undisturbed samples. The validity of the results is subordinate to the condition that the field installation of neutron and/or Time Domain Reflectometry (TDR) probes (Hillel, 1998) or taking of samples does not disturb the porous medium (Basile et al., 2003, 2006). Both in field and laboratory experiments the system to be characterised usually concerns very simple one-dimensional flow processes of wetting or drainage. Appropriately positioned measuring devices allow, in time and at specified depths, water contents θ and h to be recorded. With simultaneous measurements of θ and h it is possible to obtain at various points in the flow domain the functions $\theta(h)$, while conductivity values are determined by means of Darcy's law, inferring from the evolution of θ and h profiles, the gradients of the potential and water flux density at various depths (Hillel, 1998).

In the following, some methodologies will be illustrated which are widely used for hydrological characterizations of unsaturated porous media.

3.1 The evaporation method

According to this method, the determination in the laboratory of the hydraulic properties of soil can be made by submitting undisturbed soil samples to a process of evaporation of the upper surface, having taken care to seal off the lower one in order to prevent water-loss from the bottom (Figure 1).

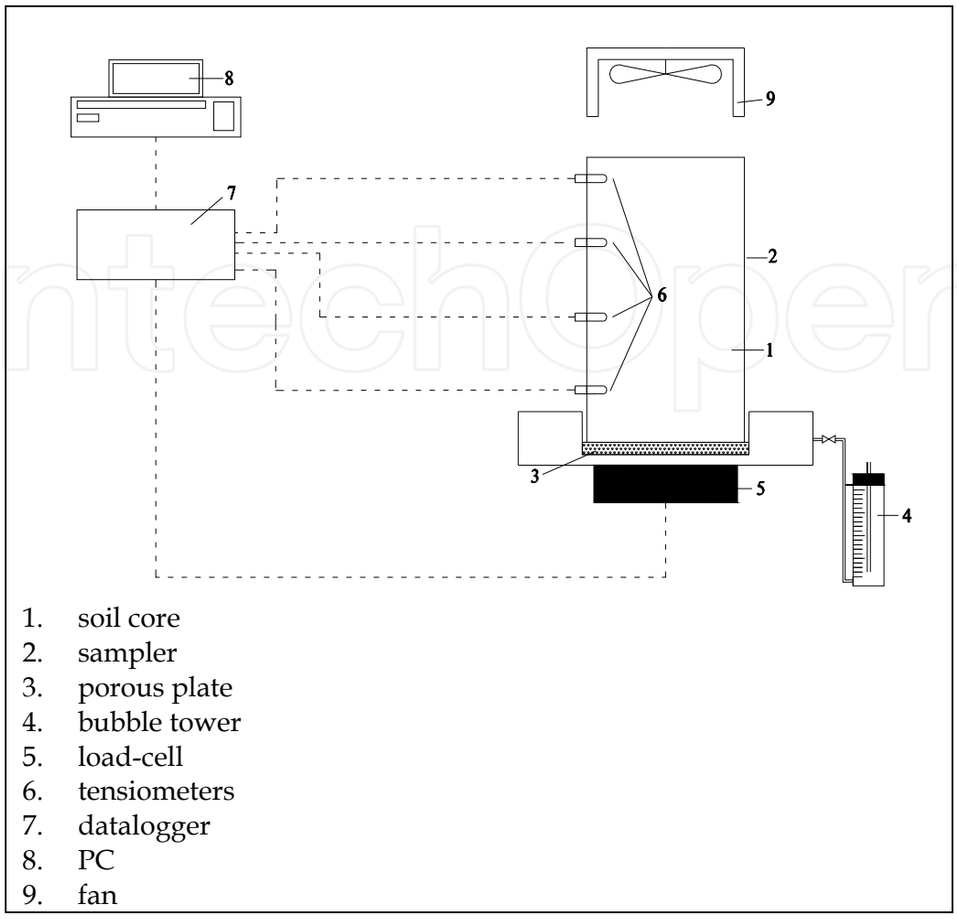

1. soil core
2. sampler
3. porous plate
4. bubble tower
5. load-cell
6. tensiometers
7. datalogger
8. PC
9. fan

Fig. 1. Scheme of experimental setup of the evaporation method

This method was originally developed by Wind (1968) and subsequently used by Boels (1978) and Tamari et al. (1993).

The soil samples, after depth saturation, can be dried under thermoregulated conditions employing a small fan with the same diameter as the sample and positioned about 10 cm above its upper surface.

Following the starting of the fan, a constant evaporation flow is rapidly determined, the value of which can be varied within certain limits by regulating the air-flow which strikes the upper surface of the sample.

During the transient state, simultaneous measurements of the weight P of the sample can be taken, using strain-gauge load cells with a measuring range from 0 to 6 kg and precision ± 1 g and of potential h to 4 or 5 depths z of the sample. The measurement of the potential values is effected by boring on the sampler wall a fixed number of holes, into which are then inserted miniaturized tensiometers with a porous septum of sinterized glass (10 mm diameter and 30 mm length, bubbling pressure at 500 hPa) joined to pressure transducers.

The measuring and recording of the data can be carried out by the data control and acquisition system, driven by a numerical calculator, and the depletion process is interrupted at the observation of the entrance of air into two tensiometers.

Following this, with the aim of extending the curve θ(h) to lower potential values, the sample is removed and, after having been broken down into sections of depth equal to 2 cm, is submitted to further draining on the membrane plate apparatus (Klute, 1986).

The measurements of evaporation flows and of potentials at different depths permitted the evaluation of both the retention curve θ(h) and the conductivity curve K(θ).

In fact, assuming that the sample can be characterized by a single equation:

$$\theta = f(\mathrm{h}) \tag{6}$$

and indicating with ΔP_t, the weight of evaporated water from the beginning of the transient until time t we have:

$$\Delta P_t = A\int_0^L \gamma\left[\theta(z) - \theta_0(z)\right]dz \tag{7}$$

in which $\theta_0(z)$ indicates the initial distribution of water content, and A the cross-section of the sample.

Equation (7), then, taking into account equation (6), can be set out in the form:

$$\Delta P_t = A\int_0^L \gamma\left[f\left(h(z)\right) - f\left(h_0(z)\right)\right]dz \tag{8}$$

If finally, the sample is divided into n strata of range Δz ,and if we assume that the measured h as taken by each tensiometer correspond to the mean values of the strata, (equation 8) can be approximated by:

$$\Delta P_t \cong A\gamma\sum_i^n\left[f\left(h_{t,i}\right) - f\left(h_{0,i}\right)\right]\Delta z \tag{9}$$

in which $h_{t,i}$ indicates the potential h measured to time t by the tensiometer of stratum *i*.

Following the suggestions of Boels et al. (1978) the equation θ=*f*(h) can be approximated with a polygonal with k vertices for which, when the axes h_j^* of the vertices are fixed, the equation θ=*f*(h) will be sectionally linear and can be defined once the values θ_j^* of water content corresponding to potentials h_j^* are known.

Therefore, once the weight variation ΔP_t and the potentials $h_{t,i}$. and $h_{0,i}$ are known , and the values of h_j^* fixed, equation (9) can be reduced to a linear equation in the unknown quantities θ_j^* . The determination of the values θ_j^* is possible if the potentials and weights are experimentally estimated at different times, and if the system of linear equations, obtained by writing (9) at least for K values of *t*, is resolved.

The precision of these evaluations can be increased within certain limits by raising the number of equations and therefore of the number of measurements.

The choice of the values h_j^* will be arbitrary, but in each case, in order to obtain a uniform approximation of the tension curves through the entire range being surveyed it is necessary

to have the values $h_{t,i}$ when measured, fall uniformly into all the intervals between two values h_j^* .

To make practicable the evaluations of θ_j^* a code can be prepared, which is able automatically to fix the most convenient coordinates h_j^* of the vertices of the polygonal θ=*f*(h) and to resolve the system of equations (9) by minimizing the sum of the squares of the residuals.

Once the law θ(h) had been obtained using the foregoing procedure, and using the potential profile h(z,t), it is possible to turn to the water content profiles θ(z,t) and to calculate the conductivity K in the function of θ, using the instantaneous profile method in the way demonstrated earlier (Hillel, 1998).

3.1.1 A case study

In this section, we refer to a study directed at the hydraulic characterization of a silty-loam soil of the southern Italy. The soil develops on a recent alluvial formation of material of marine and fluvial origin, containing sandy clay lying on gravel beds. With reference to the 7th approximation proposed by the Soil Survey Staff of the U.S. Department of Agriculture, it is an association in which predominate fluvents vertic and vertic soils, with the former represent most strongly.

As to the texture, it is made up of silty-loam soils (sand 25%, silt 51%, clay 24%) to a depth of ≈110 cm, changing to loam/sandy-loam (sand 60%, silt 28%, caly 12%) at depths over 110 cm.

Six measuring sites were individuated which, taking into account preliminary inquiries into the structure of spatial variability of the hydraulic characteristics, may certainly be considered spatially independent (Gajem et al. 1981).

On each site, by means of the digging of a pit to the depth 10-40 cm, 40-60 cm and 60-80 cm, samples of undisturbed soil of diameter 80 mm and height variable between 140 and 160 mm, were taken. For each sample, we determined texture, bulk density, hydraulic conductivity at saturation point, and curves θ(h) and K(θ).

The percentage of sand, silt and clay, in keeping with the scheme proposed by the ISSS, was determined using the densimetric method (Day, 1965). Bulk density was obtained by drying the soil samples in an oven at a temperature of 105° C, basing the calculation on soil weight and on the volume of the cylindrical container.

The determination of the hydraulic properties of the soil samples can be made using the evaporation method.

In Figure 2 is presented, by way of example, the time-flow values of the evaporation of water volume at the top of samples no.34 and no.40, taken from the depths z=10-40 cm and z=60-80 cm respectively.

The evaporation process is determined by external energy, combined with the capacity of the soil to make available to the surface of evaporation the relative volumes of water.

Therefore, in general the process evolves in two distinct phases, of which the first is characterized by constant flow which depends only on the difference in vapour concentration between the air and the soil surface and on the laminar boundary resistances of the air.

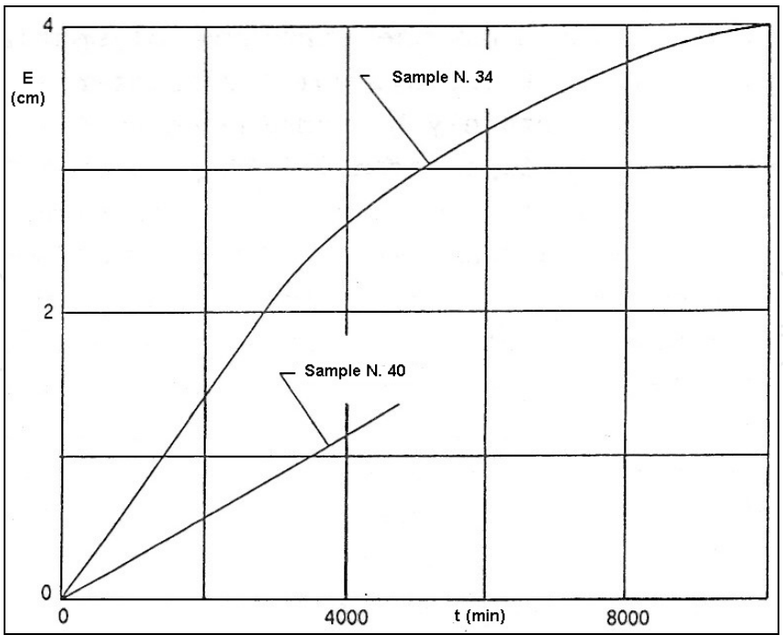

Fig. 2. Relation of cumulated evaporation E to time, for samples 34 and 40

When the soil surface reaches a level of water content such as not to permit the carriage of adequate water from the lower layers, the process becomes characterized by a reduction in time of evaporation flows, which is ever more marked by the reduction in water content.

These two phases are clearly visible in Figure 2, in which the evaporation process in sample no.34 was protracted for longer values of time.

From the graph, it can be seen that the flow of initial evaporation from sample no.40 is reduced. In fact it was necessary, in the case of samples characterized by low conductivity at saturation-point, to reduce the ventilation flow so as to avoid over-rapid depletion of the upper layers, which leads to potential profiles characterized by gradients which are too high at the surface and which cannot therefore be evaluated to an acceptable approximation.

However, in the tests it was necessary, depending on the particular characteristics of the samples, to regulate the flow of air so that water movement within the soil be sufficiently well distributed.

In Figures 3 and 4, for the two samples above mentioned, the potential values at different measuring depths are presented. From the graphs, we see that the potentials are clearly well differentiated from one another and that they evolve regularly in time, in such a way as to facilitate processing.

The results of the formulations carried out for all the samples according to the methodology illustrated allowed us to arrive at the presentations $\theta(h)$ of Figures 5 and 6, in which are shown the points specifying the vertices of the polygonals with which the retention curves were approximated.

Figure 5 in particular refers to samples taken from a depth of 10-40 cm and shows how the values of maximum water content are arranged in a band between 0.46 and 0.52, while for h equal to -250 cm, the values of water content are between 0.32 and 0.38.

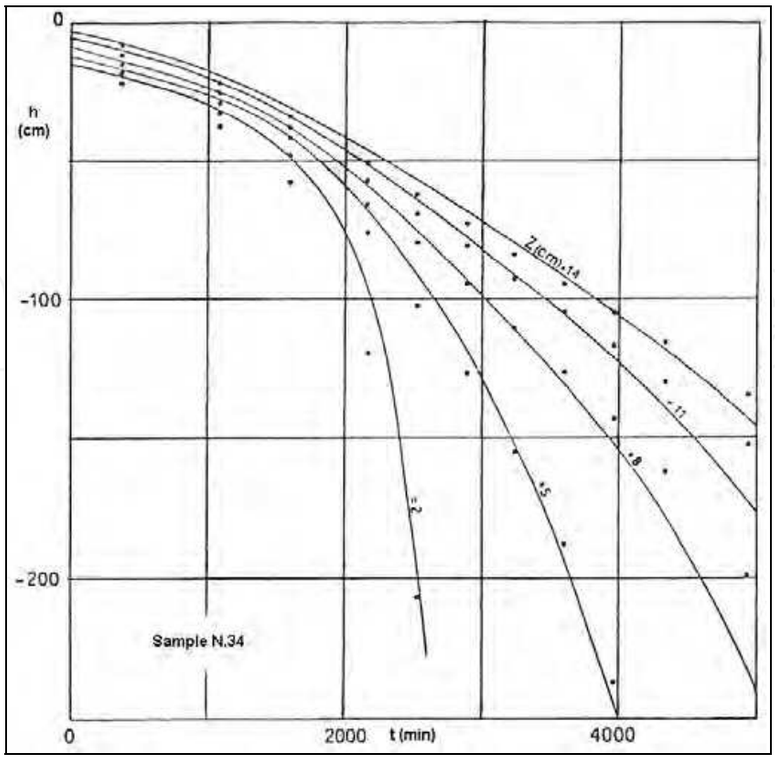

Fig. 3. Measured (circles) and calculated (solid lines) h(t) data for different depths of sample 34

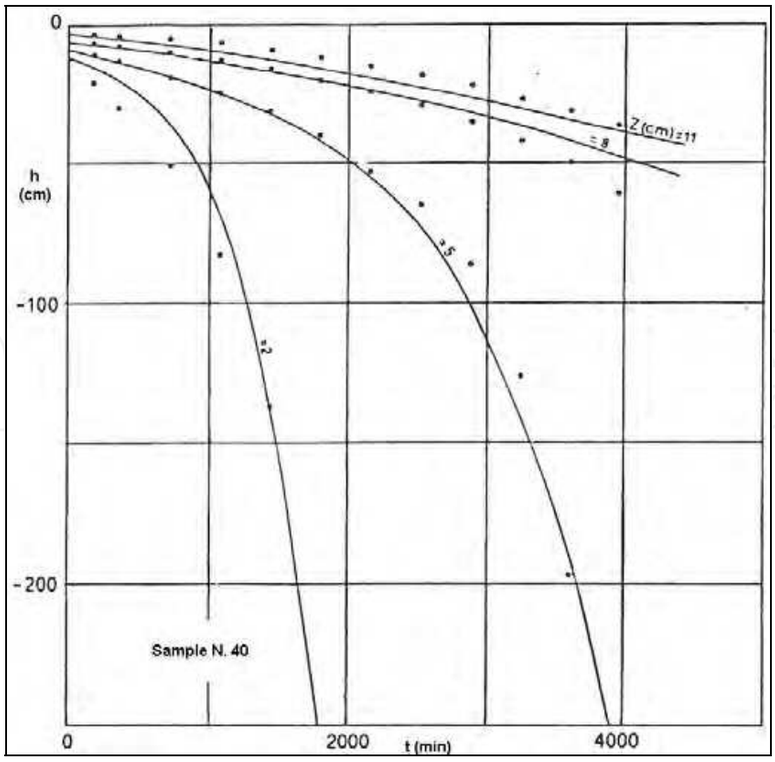

Fig. 4. Measured (circles) and calculated (solid lines) h(t) data for different depths of sample 40

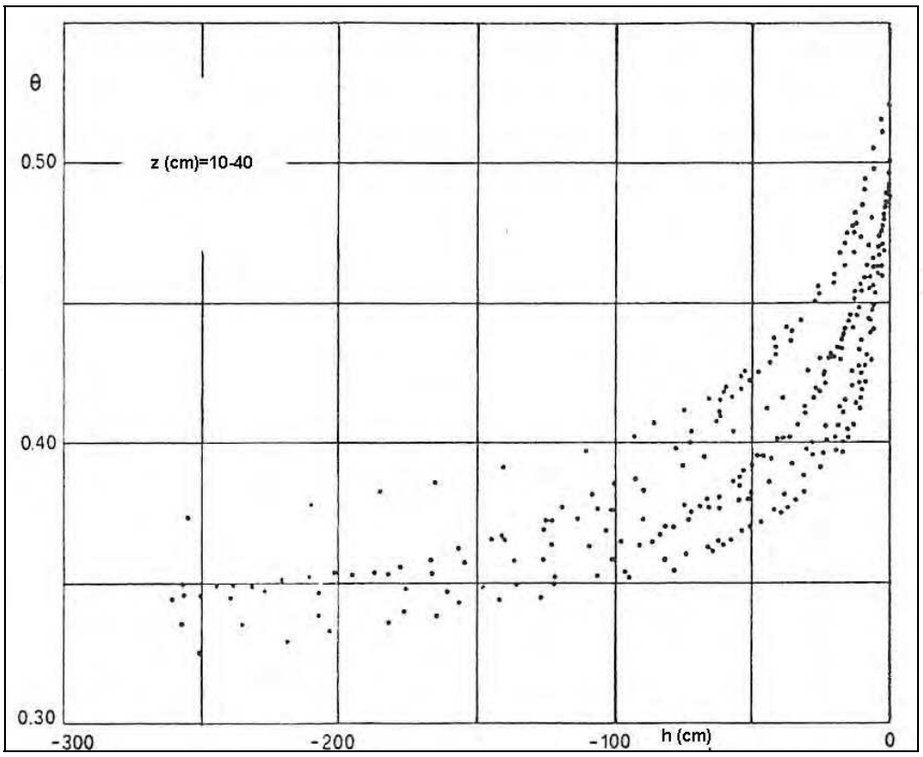

Fig. 5. Pooled soil water for all samples of selected depths 10-40 cm

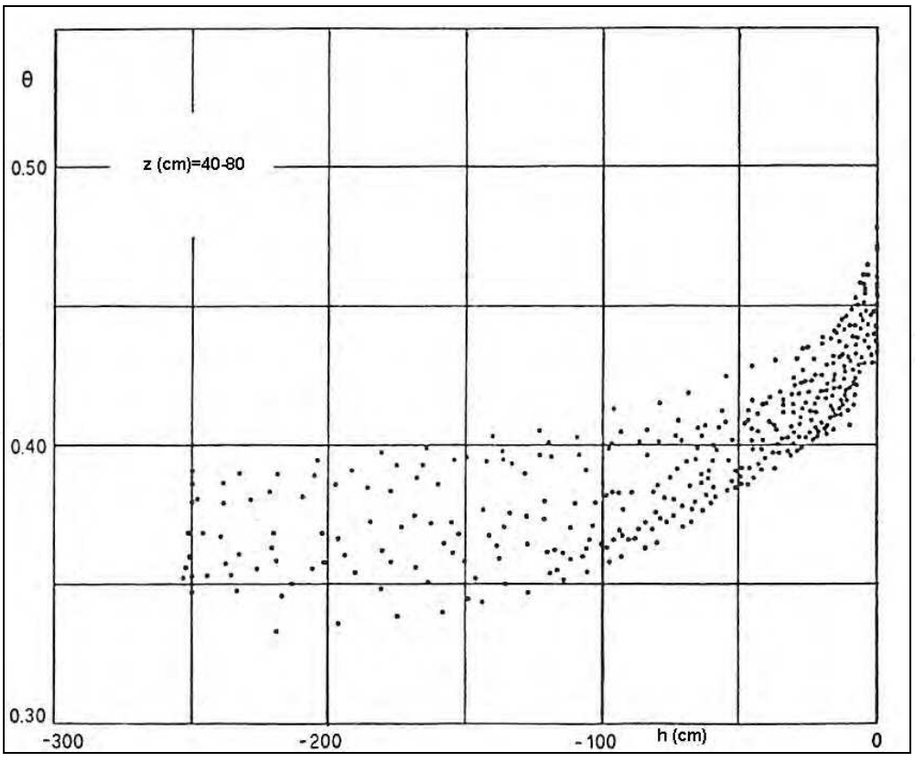

Fig. 6. Pooled soil water for all samples of selected depths 40-80 cm

Figure 6 refers to all remaining samples taken at a-depth of 40-80 cm, in so far that it was not possible to make distinctions between them. From the graph, it can be seen that the values of maximum water content are lower, and fall within a narrower band than those of Figure 5.

For a more practicable comparison, in Figure 7 are presented the mean retention curves for the two depth bands and the range of values of θ, into which it is expected that 68% of the water content will fall. The comparison shows how the mean maximum water content is equal to 0.50 for the surface samples and equal to a little over 0.45 for the deeper layer which, at potential values of -250 cm, is characterized, on average, by higher water content than the superficial layer.

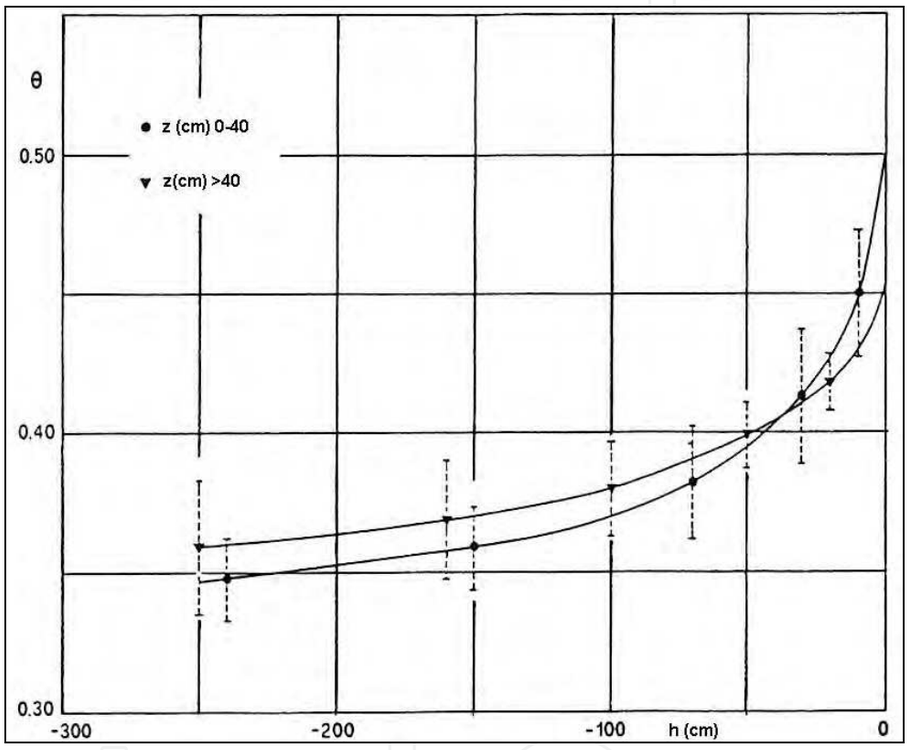

Fig. 7. Mean soil water retention curves

The hydraulic conductivities relative to the two ranges of depth, calculated using the methodology above described, are presented in Figures 8 and 9 in the function of water content. It can be seen that, as for all the samples, water conductivity is considerably reduced with a diminution of water content and that, despite there being a notable dispersion of points, slightly lower conductivities correspond to the greatest depths.

This test methodology was shown to be highly practicable, in that it did not call for the use of sophisticated equipment. The only evaluations necessary were of the weight of the samples and of the potentials at different depths.

To be able to test what the measurements mean and their precision, in view of one of their possible uses in simulation models, calculations were then carried out using the mathematical model, established in order to facilitate the study of evaporation processes in

bare soil. The model was used to reconstruct the transient of evaporation effected during the tests, by attributing to each sample the hydraulic properties determined using the methodology previously illustrated.

With the aim of greater practicability, the analytic expression proposed by van Genuchten et al. (1980) was applied to the retention curve θ(h); while the conductivity curve was approximated with an exponential function at two parameters. The parameters shown in the above-mentioned equations were then determined by adapting, through the optimization method, the analytic curves to the experimental data.

The results of these calculations were shown to be quite similar to the measurements taken during the tests. In particular, continuing to refer to sample nos. 34 and 40, in Figures 3 and 4, together with the curves measured experimentally, are shown the results of the numerical reconstructions carried out. In these graphs it can be seen that the dispersion of the points is modest: this can, however, be attributed to the imperfect homogeneity of the samples.

Therefore the verification calculations we carried out show how the test method employed is sufficiently precise for application in mathematical models.

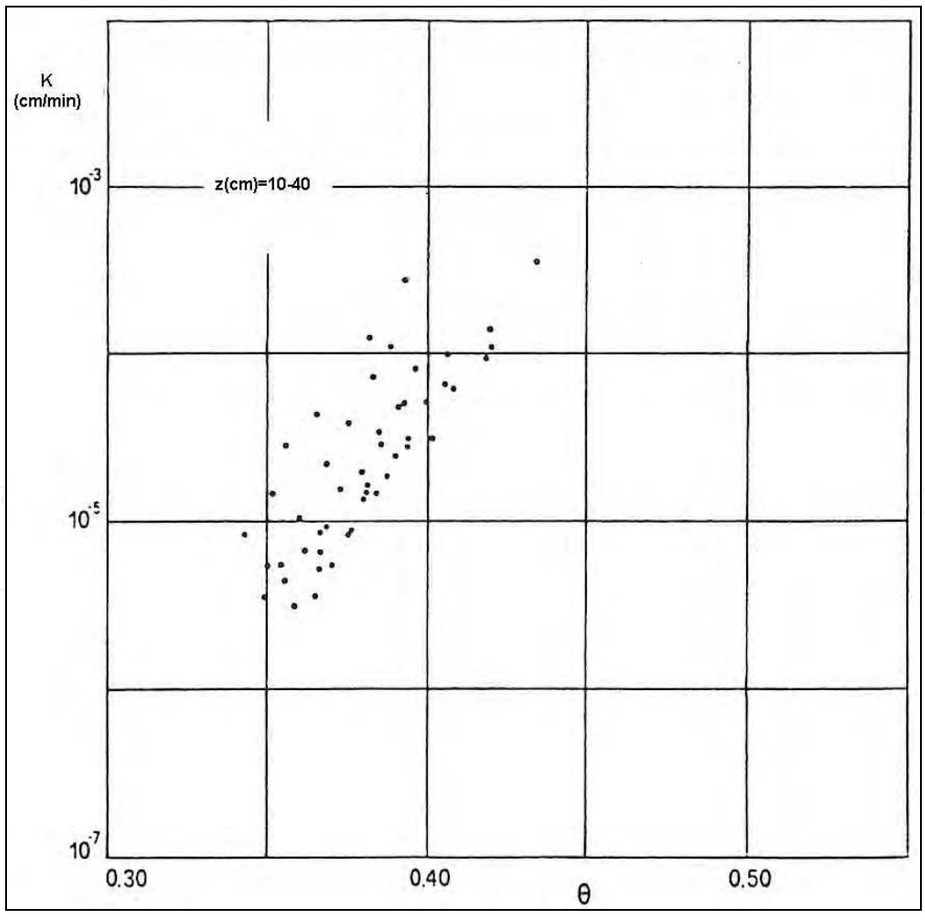

Fig. 8. Pooled hydraulic conductivity data for all samples of selected depths 10-40 cm

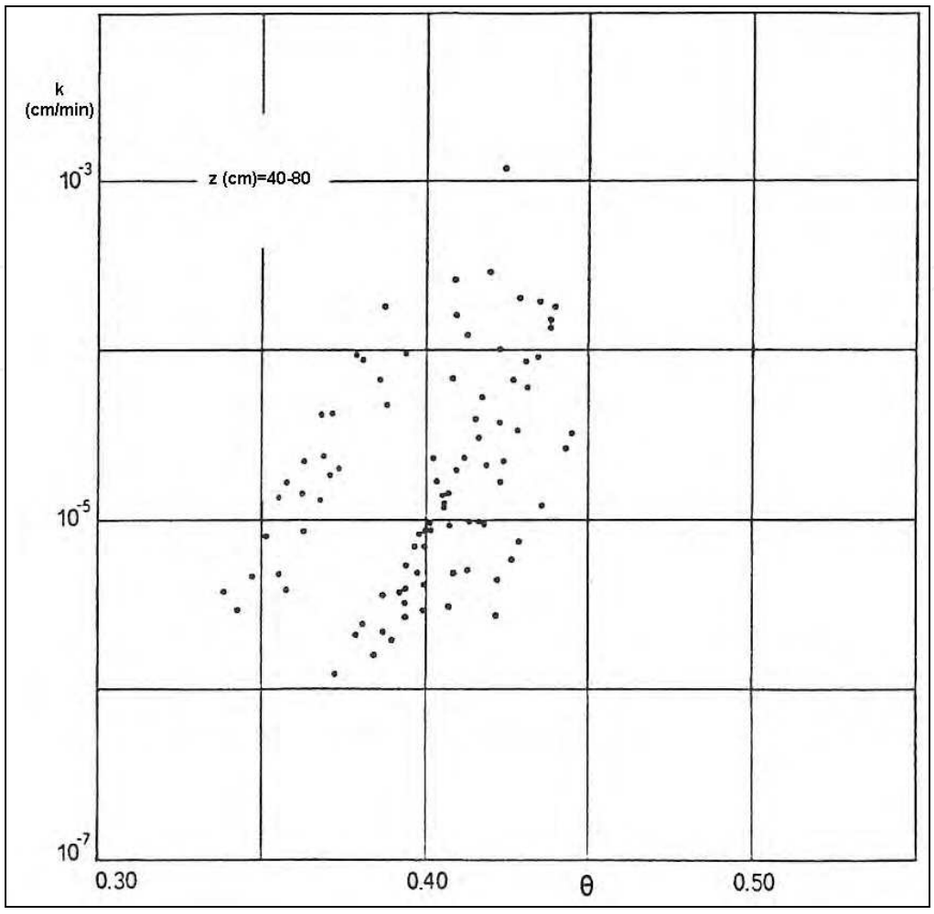

Fig. 9. Pooled hydraulic conductivity data for all samples of selected depths 40-80 cm

3.2 Internal drainage method

The water retention function θ(h) is generally determined directly in the laboratory by exposing undisturbed soil samples to wetting and drying cycles and carrying out measurements in equilibrium conditions or in the field by measuring several times concurrently the water content θ and the potential h (Klute et al. 1986).

It is far more difficult and laborious to determine hydraulic conductivity, in that it varies by several orders of magnitude, not only for different soils, but also for the same soil, as a function of water content. Moreover, for some soils laboratory methods are inadvisable: global characterisation is required with the use of direct measuring methods in the field.

For field determinations, during a drainage process, the liquid phase is almost always monitored by tensiometers which allow water potential h to be measured at different depths and by using TDR and/or neutron probes to measure the water content in volume θ. The data thus acquired are processed to define, for each measurement depth, the corresponding retention curve θ(h). Moreover, with the availability of profiles of potential h(z) and water content θ(z) the conductivity curve K(θ) can be directly obtained with the instantaneous profile method (Watson, 1966).

Such field tests are both time-consuming and burdensome, partly due to the difficulty with the automation of data collection. However, they provide representative results for the scale of measurements and, in some situations, are the only results achievable (Hillel, 1998).

3.2.1 Theory

Profiles of water content $\theta(z)$ and potential $h(z)$ allow us to determine hydraulic conductivity with the instantaneous profile method. Indeed, by integrating the differential equation of one-dimensional water flow in unsaturated media:

$$\frac{\partial \theta}{\partial t} = \frac{\partial}{\partial z}\left[K(\theta)\left(\frac{\partial h}{\partial z} - 1\right)\right] \tag{10}$$

between z=0 and depth Z and assuming that there is zero flow at the soil surface, we obtain:

$$\int_0^Z \frac{\partial \theta}{\partial t} dz = \left| K(\theta)\left(\frac{\partial h}{\partial z} - 1\right)\right|_{z=Z} \tag{11}$$

hence:

$$\left|K(\theta)\right|_{z=Z} = \frac{\int_0^Z \frac{\partial \theta}{\partial t} dz}{\left|\frac{\partial h}{\partial t} - 1\right|_{z=Z}} \tag{12}$$

Equation (12), expressed in discrete form, allows hydraulic conductivity to be determined by using experimental data. Indeed, with reference to a time interval t_{i+1}-t_i, and corresponding variations in water content θ_{i+1}-θ_i, we have as follows:

$$K\left(\bar{\theta}\right) = \frac{\int_0^Z (\theta_i - \theta_{i+1}) dz / (t_{i+1} - t_i)}{\left|\frac{\partial h}{\partial z} - 1\right|_{t=(t_{i+1}-t_1)/2}^{z=Z}} \tag{13}$$

where $\bar{\theta}$ may be determined using the relation:

$$\bar{\theta} = \frac{1}{2}\left(\theta_{i+1}(Z) - \theta_i(Z)\right) \tag{14}$$

and the derivative $\partial h / \partial z$ may be evaluated with finite differences from the measurements of potential h.

3.2.2 A case study

In this section we refer to a survey to characterize a volcanic topsoil hydraulically determining $K(\theta)$ and $\theta(h)$ based on the instantaneous profile method.

The experimental field soil, which is located at the Ponticelli-site (nearby Naples, Italy), is a sandy soil (sand 80%, silt 12%, clay 8%), pedologically classified as andosol. The main feature is that the soil is macroscopically homogeneous up to 0.80 m, with a layer of finer textured (loamy) soil at 0.80÷1.00 m. Measurements of the soil bulk density ρ up to 1.00 m (with 0.30 cm depth intervals) at various locations across the field had mean and standard deviation equal to 1.01 g/cm^3 and 0.13 g/cm^3), respectively.

For the purposes of soil hydraulic characterization, in terms of the water retention θ(h) and hydraulic conductivity curves K(θ), a 40x7m^2 plot was set up (Figure 10). On a side transect of the plot 120 three-wire steel probes were installed at different depths (z=0.30, z=0.60 and z=0.90 m), spaced 1 m apart, to measure water content with the time domain reflectometry method (TDR) (Topp et al., 1980). Along a parallel transect 0.50 m from the probe transect 120 tensiometers were installed to measure water potential h.

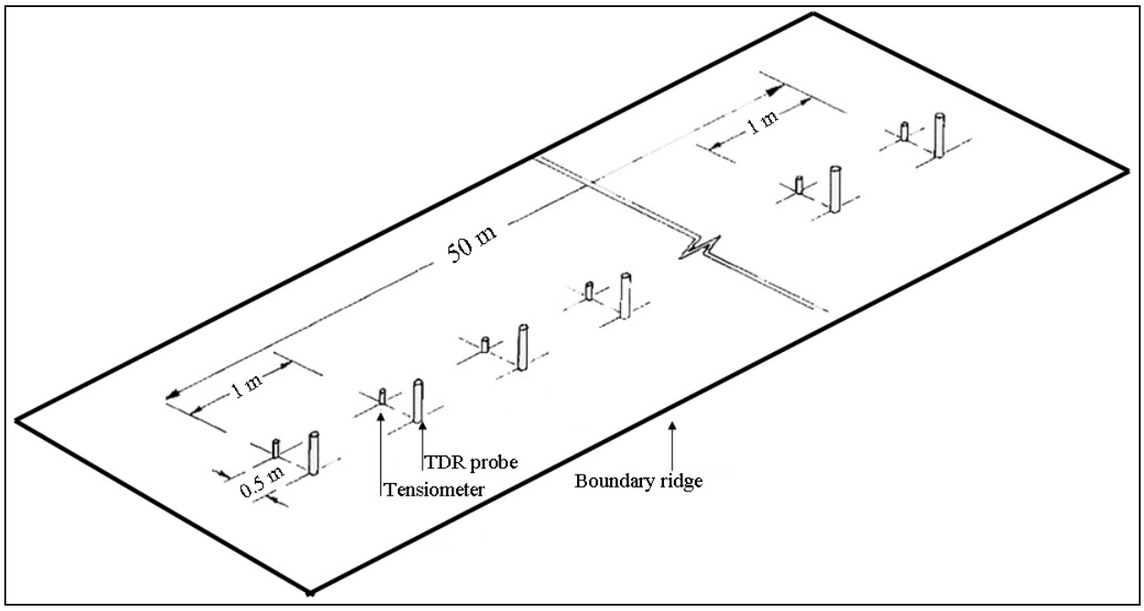

Fig. 10. View of the experimental plot displaying relative position of TDR probes and 0.3 m depth tensiometers.

As commonly used for field determination of soil hydraulic properties, when infiltration was completed, a drainage test was then carried out. With reference to the instantaneous profile method, potential h and water content θ are measured at the same time during a process of redistribution of the liquid phase, with evaporation and rainfall infiltration prevented at the soil surface by a plastic sheet.

Measurements of water content and potential were conducted in 12 campaigns and interrupted about 80 days from the end of infiltration, when the drainage process was evolving so slowly as to make it fruitless to continue measurements.

To increase the method's rapidity and versatility, water content and potential were measured by connecting the TDR probes and tensiometers to new-generation portable testers (Hopmans et al 1999; Carlos et al, 2002): TDR 100 testers (Campbell Scientific Inc, Logan UT) and a tensimeter-microdatalogger (Skye Instruments Ltd., UK). The calibration

curve of the TDR probes was determined with the method proposed by Regalado et al. (2003) for volcanic soils.

At the end of the test, at each measuring site, at the average profile depth of 0.30 m soil hydraulic conductivity was measured at saturation K_s with the constant-head well permeameter technique (Amoozegar and Warrick, 1986). At the same depth, disturbed soil samples were taken to determine texture with the densimetric method (Day, 1965).

With reference to one of the profiles examined (no. 5) along the transect, Figures 11, 12 and 13 illustrate the extent of the transients induced in the porous medium during the test.

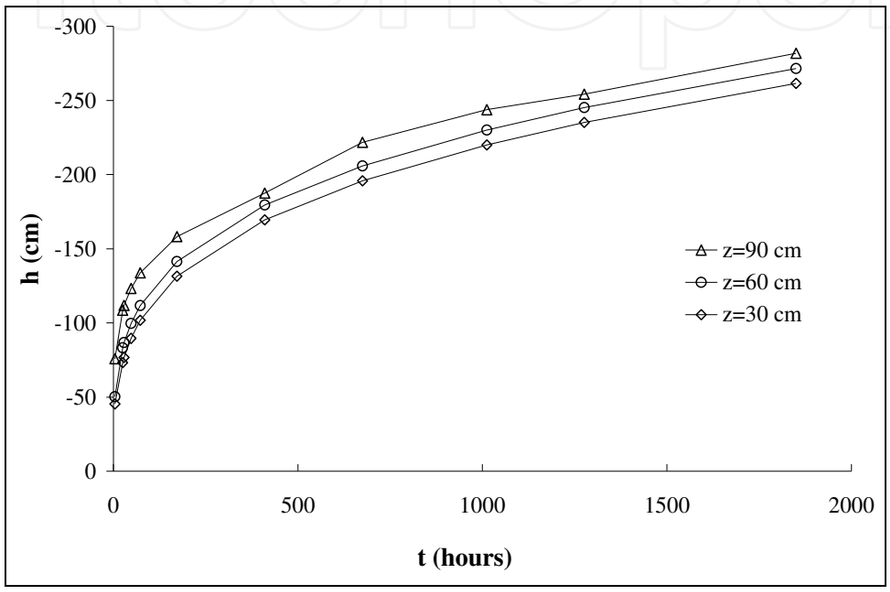

Fig. 11. Field values of h(t) for the drainage transient of profile 5

Water potential measurements (Figure 11) at various depths show that the potentials are sufficiently differentiated and evolve in time with regularity so as to permit straightforward calculation of the gradient.

Total hydraulic potential H distributions with depth z and for some test times are reported in Figure 12. The continuous lines indicate that the profiles obtained may be described with good approximation by a linear relation.

Finally, θ is plotted against time t (Figure 13). After the rapid fall in water content during the first few days of drainage, θ values continue to drop significantly and at the end of the test appreciable reductions in water content over time are found for all depths. This shows that the soil in question has a considerable natural drainage capacity and that it is in practice impossible to define correctly the so-called "field water capacity" of the topsoil.

The elaboration of the whole data pool allowed us to obtain the h(θ) and the K(θ) reported in Figure 14a and 14b, respectively. The scatter of θ(h) points in Figure 14a is contained in a fairly narrow bound and shows marked homogeneity of the soil in question. By contrast the K(θ) values in Figure 14b show greater dispersion, even if somewhat restricted compared to those from other studies (Jury et al., 1991).

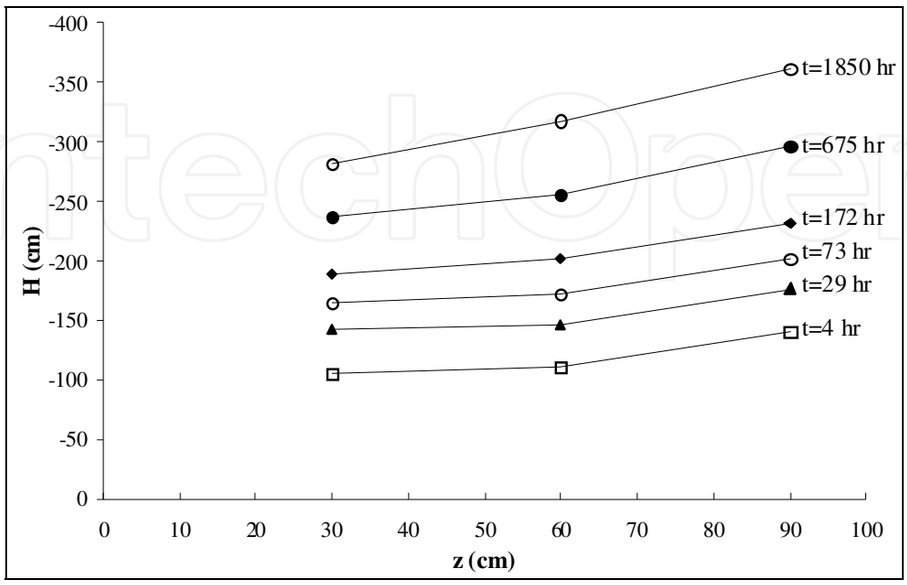

Fig. 12. Field values of H(z) for different time relative to the drainage transient of profile 5

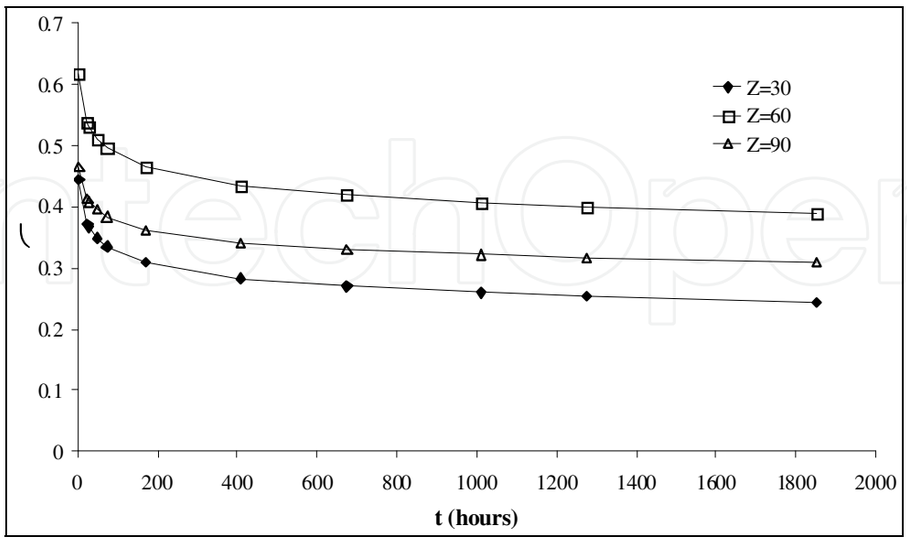

Fig. 13. Field values of θ(t) for the drainage transient of profile 5

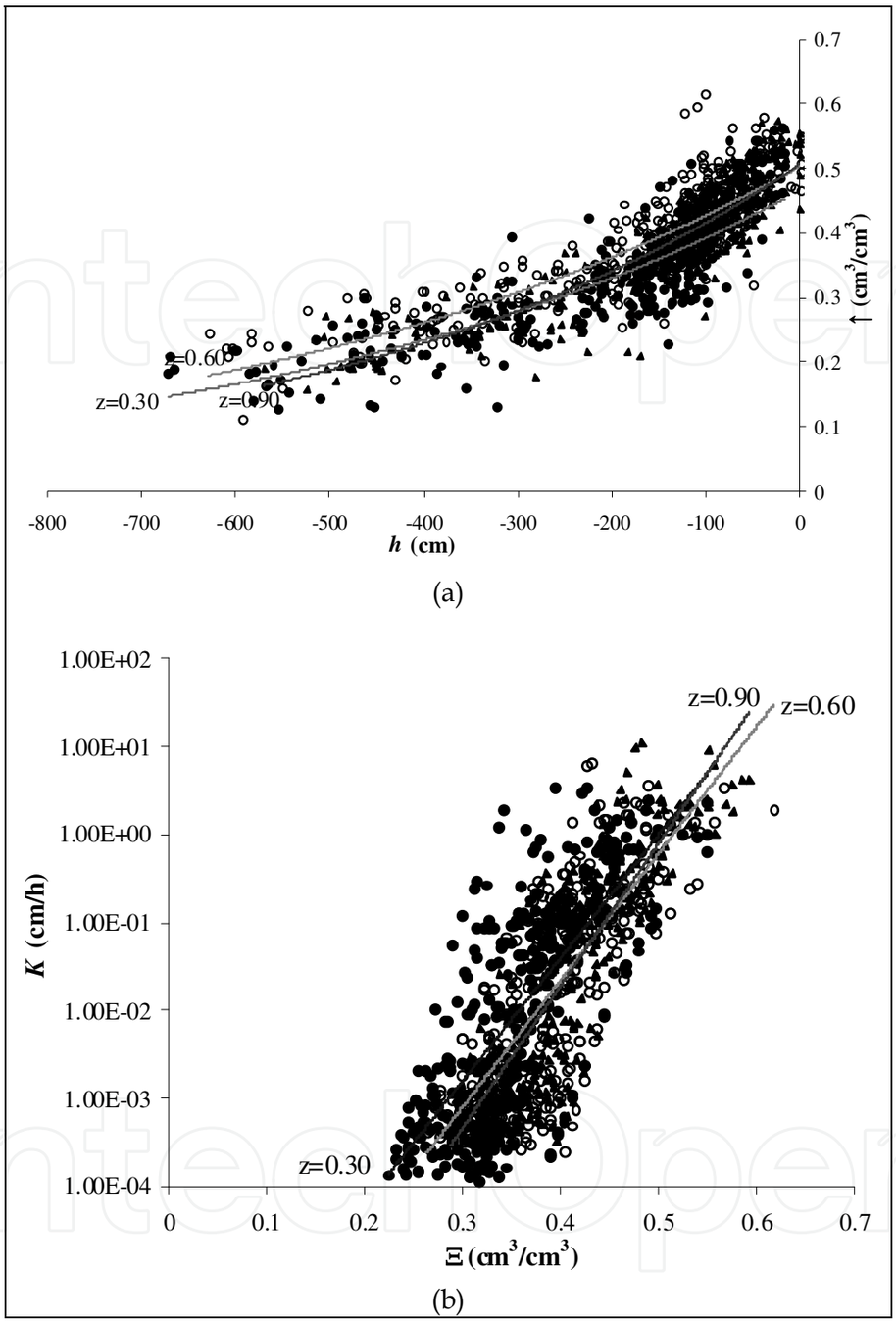

Fig. 14. a. Scatter of θ(h) and b. of K(θ) values detected at various depths of the soil profiles along the transect

3.3 Simplified analysis of internal drainage experiments

To make the measurements less laborious, for determining only hydraulic conductivity, simplified methods have been proposed (Libardi et al., 1980; Chong et al., 1981) whereby only one variable, θ or h, needs to be measured in the field, during the drainage process.

Hydraulic conductivity is evaluated by making simplifying hypotheses on the distribution of water potential gradients during the experiments and by assigning analytical expressions to relations K(θ) or K(*h*) and to the laws by which θ or h vary in time.

The above expressions, generally with no more than 3 parameters, have been confirmed experimentally for very different soils, albeit with a homogeneous profile (Nielsen et al., 1973; Dane, 1980; Sisson and Van Genuchten, 1991), whereas they have been found inadequate in the case of soils characterized by successions of numerous strata with different physical characteristics (Schuh et al., 1984; Jones and Wagenet, 1984; Ahuja et al., 1988).

3.3.1 Theory

The methods of Libardi et al. (1980) and Chong et al. (1981) for calculating the conductivity relation are based on Richards' differential equation which, for one-dimensional vertical flow has the form:

$$\frac{\partial \theta}{\partial t} = \frac{\partial}{\partial z}\left[K(\theta)\frac{\partial H}{\partial z} \right] \tag{15}$$

Furthermore, the following simplifying assumptions were made:

1. The soil water flux at time t=0 is constant in the whole soil profile ($0 \le z \le L$), and for t > 0 at the soil surface the zero flux condition occurs.

For these cases, by integrating equation (15) we obtain:

$$\int_{z=0}^{Z=L} \frac{\partial \theta}{\partial t} = \left[K(\theta)\frac{\partial H}{\partial z} \right]_{z=L} \tag{16}$$

If θ^* represents the average water content of the profile, up to the maximum depth *L*, equation (16) is reduced to:

$$L\frac{d\theta^*}{dt} = \left[K(\theta)\frac{\partial H}{\partial z} \right]_{z=L} \tag{17}$$

2. The average relationship between θ^* and the water content $\theta(L,t)$, at depth is assumed to the form:

$$\theta^* = a\theta + b \tag{18}$$

where *a* [L] and *b*[L] *are* empirical constants.

3. Between the hydraulic conductivity k and water content θ, we assume the following exponential relation:

$$k(\theta) = k_0 \exp\left(\beta(\theta - \theta_0)\right) \tag{19}$$

where β[L^3,L^{-3}] is a constant, and K_0 and θ_0 are the hydraulic conductivity and water content values at the beginning of the drainage process.

4. During the drainage process, the unit hydraulic head gradient is assumed to be at the greatest depth $z=L$:

$$\frac{\partial H}{\partial z} = -1 \tag{20}$$

With these assumptions, integrating equation (17) and by means of equations (18)-(20) the following relation is obtained:

$$-aL\frac{d\theta}{dt} = K_0 \exp\left(\beta\left(\theta - \theta_0\right)\right) \tag{21}$$

Where θ_0, K_0 and β apply at depth L.

To estimate K_0 and β the methods used are those proposed by Libardi et al. (1980) and Chong et al. (1981), namely: (1) θ method; (2) Flux method; (3) Lax-θ method; (4) CGA method (abbreviation for Chong-Green-Ahuja), which are briefly described below.

θ method

By integrating equation (21) with the initial conditions ($\theta=\theta_0$) we obtain for long times (t>2h):

$$\theta_0 - \theta = \frac{1}{\beta}K\ln\left(t\right) + \frac{1}{\beta}\ln\left(\frac{\beta \cdot K_0}{a \cdot L}\right) \tag{22}$$

Once a is known, the slope and the intercept with the axes of the graph of equation (22) allow parameters β and K_0 to be directly estimated.

Flux method

If the logarithms of the left-hand and right-hand members of equation (21) are considered, the following expression is obtained:

$$\ln\left|a \cdot L\frac{\partial \theta}{\partial t}\right| = -\beta\left(\theta_0 - \theta\right) + \ln\left(K_0\right) \tag{23}$$

With reference to the average values, which are more stable in the water content measurements, especially if carried out at greater depths, equation (23) may be also be expressed as:

$$\ln\left|a \cdot L\frac{\partial \theta^*}{\partial t}\right| = -\beta\left(\theta_0 - \theta\right) + \ln\left(K_0\right) \tag{24}$$

which describes a linear semi-log relationship where β and K_0 are determined from the slope and intercept, respectively.

Lax-θ method

The unit gradient hypothesis allows equation (15) to be written in the differential form:

$$\frac{\partial\theta}{\partial t} = -\frac{dK}{d\theta}\frac{\partial\theta}{\partial z} \tag{25}$$

the solutions to which are supplied by Lax (1972) and Sisson et al. (1980) for different analytical expressions for K(θ).

When K(θ) is given by equation (19), we obtain:

$$\theta_0 - \theta = \frac{1}{\beta}\ln(t) + \frac{1}{\beta}\ln\left(\frac{\beta \cdot k_0}{L}\right) \tag{26}$$

in which β and K_0 may be calculated from the slope and intercept, respectively, of (θ_0-θ) versus ln(t). It should be noted that equation (26), does not require the assumptions of equation (18) and thus it is not necessary to evaluate factor a.

CGA method

If, instead of using equation (18), we assume that there is the following type of relation between θt^* and t:

$$\theta^* = A \cdot t^B \tag{27}$$

then we obtain, instead of equation (19), the expression:

$$K(\theta^*) = -LA^{1/B}B\theta^{*(B-1)/B} \tag{28}$$

where coefficients A and B may be obtained by fitting equation (27) to experimental θ versus t data.

The β and K_0 values can be obtained from equation (28), if it is assumed that equation (18) holds and that the term $\left[a(\theta - \theta_0)\right] / \theta_0^*$ is small with respect to 1:

$$K_0 = -LA^{1/B}B\theta^{*(B-1)/B} \tag{29}$$

and

$$\beta = a\frac{B-1}{B\theta^*} \tag{30}$$

The estimates of A and B in equation (27) and of a in equation (18) thus allow us to evaluate parameters β and K_0 according to the other methods.

3.3.2 A case study

This section sets out to analyze the possibility of using limited data collected in site to determine the hydraulic properties of a volcanic soil by simplified methods proposed by Libardi et al. (1980) and Chong et al. (1981). The experimental site is located at Ponticelli (Naples, Italy). The soil profile is uniform with a moderate layering in the top metre and is classifiable as an Andosol. At the centre of the field where the trial was carried out, a

plot with dimensions of 5 m x 5 m was prepared with a boundary ridge about 0.25 m high. At the centre of the plot two aluminium tubes were inserted up to a depth of 2.0 m, for measuring at depths: 30, 45, 60, 75, 105, 135 and 150 cm, water content by means of a RONLY 701A-11-P neutron probe. To reduce instrumental variance, which essentially depends upon the random variation in the fast-neutron emission from the source, three readings per depth were averaged. The error in the volumetric water content measurements were assumed to be due mainly to the calibration curve standard error of estimate equal to 1.7%.

At a distance of 0.5 m from tube axes, nine mercury-water manometer-type tensiometers were installed with their tip at a depth of 15, 30, 45, 60, 75, 90, 105, 120 and 150 cm to register water potential. The ceramic tensiometer cups were made in our laboratory, with the following characteristics: (i) the bubbling pressure (Pa) is greater than 500 hPa; (ii) the cup conductance (C) is greater than 1.11 x 10^{-5} cm^3 s^{-1} hPa^{-1} of pressure difference across the wall; (iii) considering that the gauge sensitivity (S) is 103 hPa cm^{-3}, an instrumental time constant in water $\tau=C^{-1}S^{-1}$ may be calculated equal to 90 s.

For the purposes of the trial, the plot was ponded by applying water in excess of the infiltration rate, while an overflow pipe guaranteed a constant water depth of 0.15 m. The time required for establishing steady-state flow in the profile at all depths to 1.5 m, was about 1 week. When infiltration was completed, the surface of the plot was covered with a plastic sheet so as to prevent evaporation from the soil surface and rainfall infiltration in the soil profile (see Figure 15).

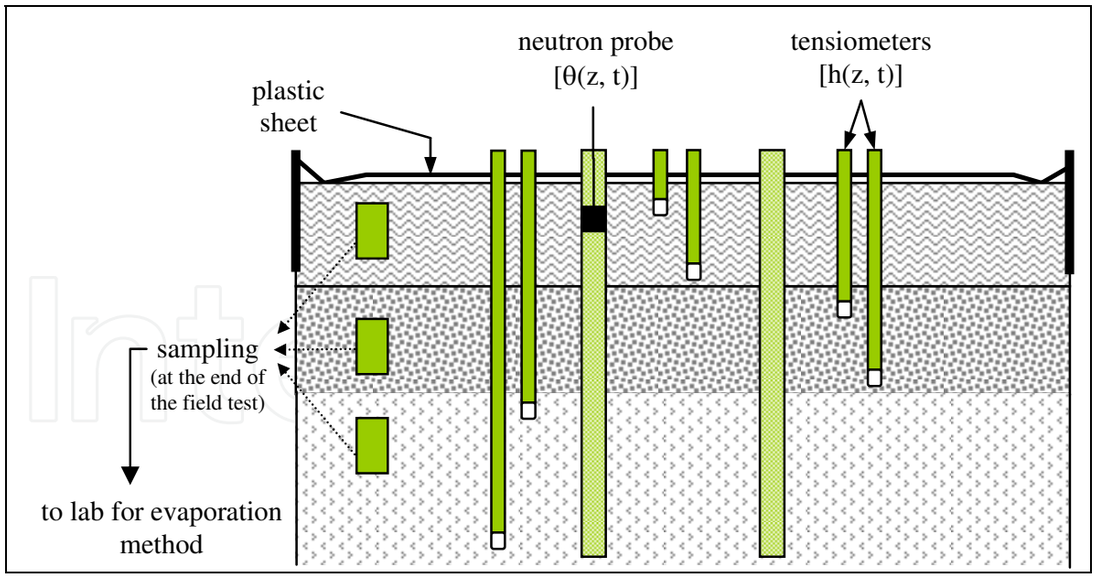

Fig. 15. Schematic of internal drainage setup

Measurements were carried out at increasing time intervals from the start of the drainage process. The water content and the potential h were always measured at the same time. Monitoring was interrupted 42 days after the end of infiltration when the drainage process was evolving so slowly as to make it pointless to continue with the experiment.

On completion of the trials at every measuring point in the profile, undisturbed soil samples were taken to determine the texture by the densimetric method (Day, 1965).

Table 1 reports the main soil physical properties measured at various depths.

Depth z (cm)	Coarse sand (2<d<0.2 mm)	Fine sand (0.2<d<0.02 mm)	Silt (0.02<d<0.002 mm)	Clay (d<0.002 mm)	Bulk density (g)cm^3)
10-20	30	50	12	8	1.15
40-50	30	53	12	5	1.10
70-80	34	48	12	6	1.09
100-110	25	63	7	5	1.09
110-120	27	60	5	8	1.09

Table 1. Texture and bulk density of the examined profile

Figure 16 shows the distribution $h(z)$ of with respect to time. The $h(z)$ curves have a regular pattern for all depths and $\partial H/\partial z \approx 0$ near the surface where evaporation was prevented by the plastic sheeting.

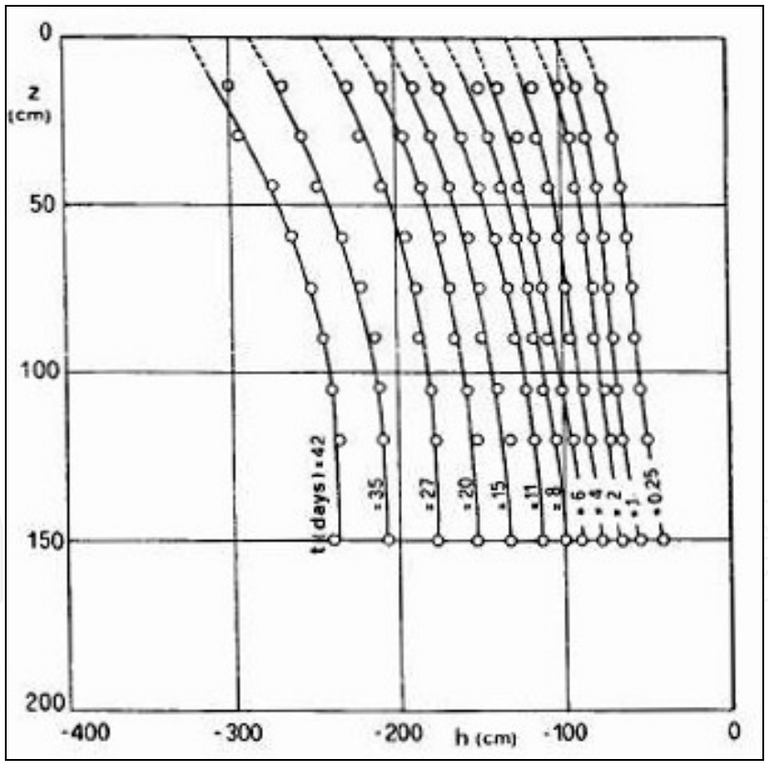

Fig. 16. Field measured h(z,t) values during drainage

The corresponding θ(z) profiles show marked discontinuities due to soil stratification (Figure 17). In the layer closest to the surface (0<z<90 cm), moderate variations of water content occur with increasing depth. Such variations then decrease as the drainage process evolves.

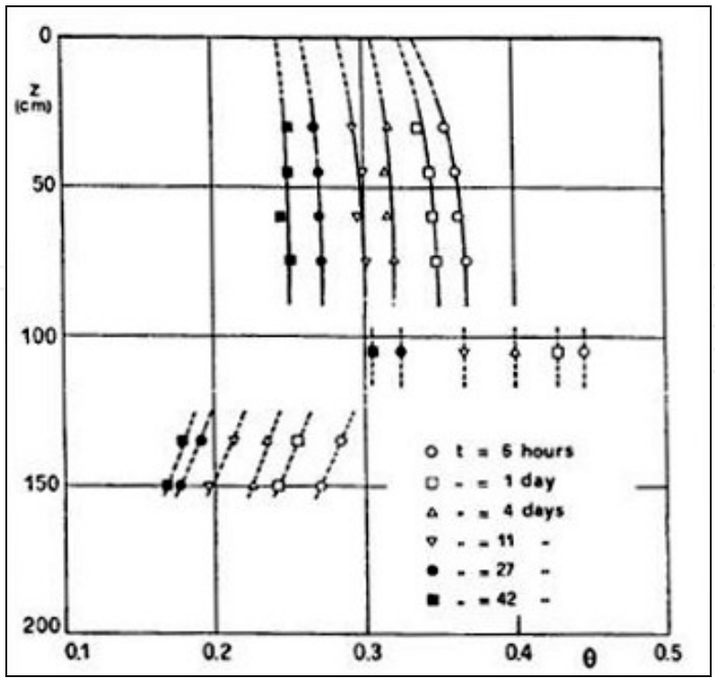

Fig. 17. Field measured θ(z,t) values during drainage

Profiles θ(z,t) for (0<z<90 cm) were used to obtain β and K_0 using each of the four simplified methods presented in equations (22), (24), (26), (29) and (30).

Table 2 reports both the parameters obtained by linear regression (equation (18)) among the average θ^* water content of the profile and the water content 0 measured at depth z=75 cm, and the results of statistical fitting of equation (27) to the observations of average water content in the profile for different time values.

$\theta^*=a\theta+b$	a=0.9476	b=0.0132	R^2=0.9995
$\theta^*=At^B$	A=0.3539	B=-0.0830	R^2=0.9758

Table 2. Parameters of equations 18 (first line) and 27 (second line) for z=75 cm. R^2 is the coefficient of determination

Figure 18-19 indicate the high agreement between observed data and the estimated regression lines. Knowledge of parameters a, A and *B*, at the preselected depth of z=75 cm, then allowed us to determine with the various methods illustrated the analytical relations which supply K as a function of θ.

Profiles *h*(*z*) and θ(*z*) were then elaborated to obtain the conductivity K in function of θ by using the *instantaneous profile method.* Integration of the θ(*z*) profiles measured for assigned values of time t, together with evaluation, by means of experimental profiles h(*z*) relative to the same times, of hydraulic head gradients, allowed us to use Darcy's Law to obtain hydraulic conductivity values K, during evolution of the drainage process. The results of the elaborations performed for depth *z*=75 cm are shown in Figure 20 which also reports the diagrams of equation (5), obtained by assigning, at each step β and K_0 values calculated respectively by equations (22), (24), (26), (29) and (30) and reported in Table 3.

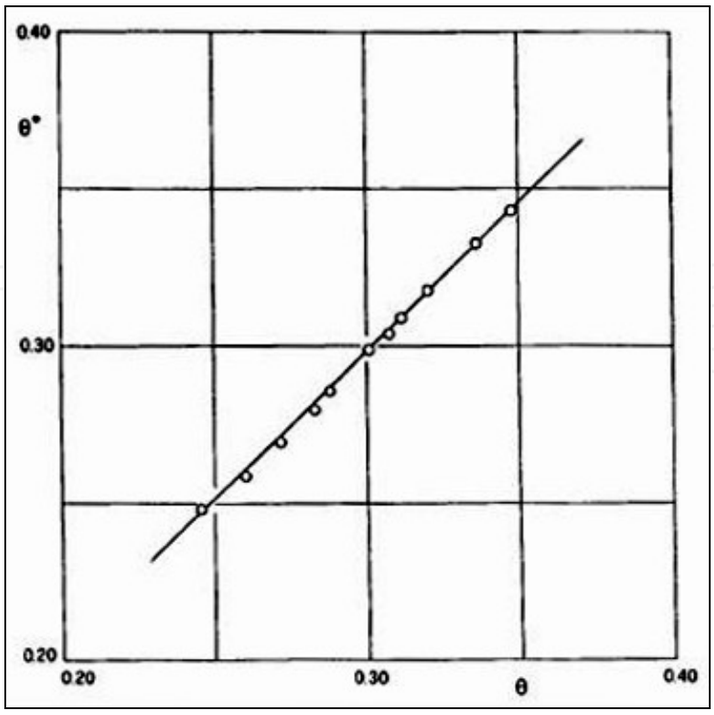

Fig. 18. Correlation between θ^* and θ at depth z=75 cm

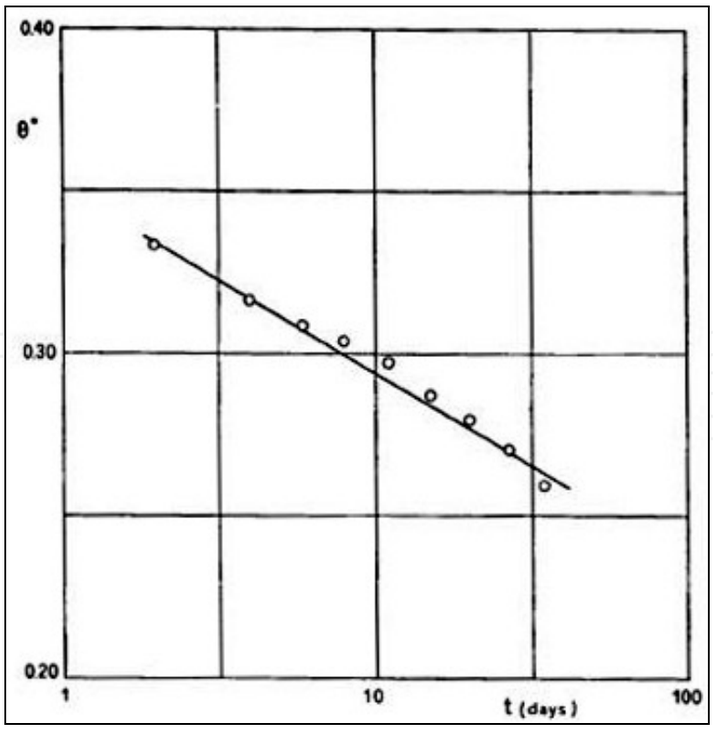

Fig. 19. Calculated curve (solid line) obtained by regression of equation 27 on measured (symbols) of water content θ^* at depth z=75 cm

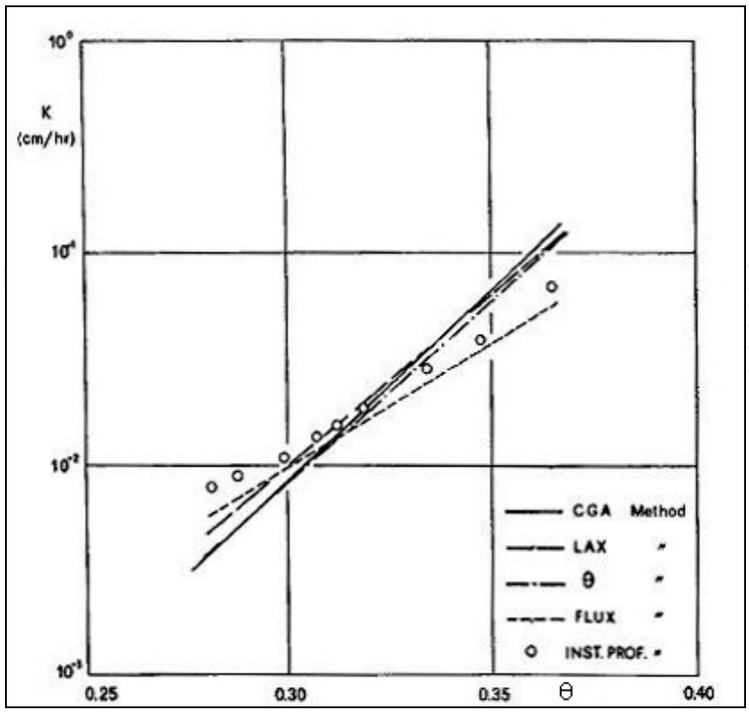

Fig. 20. Comparison between K(θ) calculated (solid line) and measured (symbols) at z=75 cm

Method	K_0 (cm/hr)	β	r
θ	1.12	37.26	0.981 [a]
Flux	1.06	27.21	1.986 [b]
Lax-θ	1.12	39.35	0.981 [a]
CGA	1.14	41.16	0.998 [c]

a Regression coefficient for $(\theta_0-\theta)$ versus ln$t$
b Regression coefficient for $\ln[aL(\delta\theta^*/\delta t)]$ versus $(\theta_0-\theta)$
c Regression coefficient for $\ln\theta^*$ versus ln$t$

Table 3. Values of parameter K_0 and β of the hydraulic conductivity function estimated by the simplified methods

Overall, the results obtained allow us to make the following comments on the soil in question:

- There is a satisfactory linear relationship between the evolution in time of moisture at the pre-selected depth and mean moisture θ^* in the profile. This confirms other experimental observations reported by Libardi et al. (1980) and by Nielsen et al. (1973) on Panoche soil.
- The unit gradient assumption, together with a postulated exponential link between K and θ (equation (19)), also consistently involves a linear relation between θ^* and $\theta(z)$.

However, no theoretical consideration allows us to justify a priori the validity of equation (27). Only the statistical fitting of the data allows us to judge the latter assumption. In our case the moisture drainage process in the profile is adequately described by equation (27).

This result also confirms those presented by Chong et al. (1981) for two Hawaiian soils with different hydraulic properties.

- The hypothesis of the unit hydraulic gradient, is not always verified (Ahuja et al., 1988). In our case Figure 21 shows, despite uncertainty due to measurement errors, that the gradient, initially close to -1, decreases slowly during the measurement period.
- It is worth noting that the various models may nevertheless also be used for hydraulic gradients different from -1 provided they are constant in time (Vauclin and Vachaud, 1987). The use of tensiometers allows us to evaluate the gradients and their possible fluctuations in time.

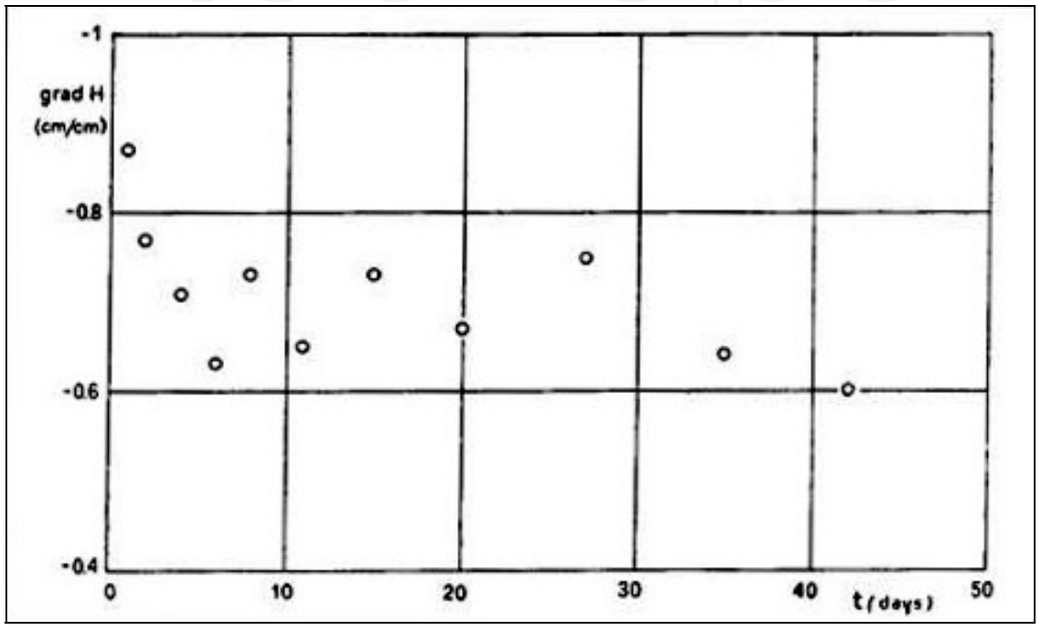

Fig. 21. Estimated field values of the hydraulic gradient during drainage at depth z= 75 cm

3.4 Disk permeameter method

Today, numerous mathematical models based on the solution of Richards' equation allow the numerical simulation of water and pollutant transfer in the vadose zone and thus may be essential instruments for assessing environmental pollution. However, the solutions offered by such models may contain considerable errors in the case of structured soils with heterogeneous pore systems which cannot be adequately described by the generally used unimodal retention and hydraulic functions. In such cases, for characterizing the flow regime, it is essential to separate the flow through macropores from the one through the soil matrix (Bouma, 1982). Recognition of this dichotomy is important because the properties of the macroporous system tend to dominate the infiltration process at and near saturation, while drainage, redistribution and root water uptake depend on those hydraulic properties which reflect the nature of the matrix.

Given the complexity of the problem, specific macropore models have recently been set up (Jarvis et al., 1991; Chen and Wagenet, 1991; Gerke and van Genuchten, 1993) which may

more simply be considered as dual-porosity models. Implementation of such models requires new technologies and, because of the ephemeral nature of macropores, a new class of experiments to be conducted, if possible, in the field, so as to obtain input data for quantifying soil hydraulic properties, macropore distribution and spatial variation of macropores.

Various methods to obtain macropore parameters have been set up, such as tracer-breakthrough curves, computerized tomography, dye-staining and sectioning (Bouma and Dekker, 1978; Warner et al., 1989). However, in most cases such methods require undisturbed soil samples and they cannot be easily transferred to the open field. More simple methods, as recently suggested, are based on measuring unconfined infiltration rates with a disc permeameter (Perroux and White, 1988; Watson and Luxmoore, 1986; Ankeny et al., 1991) or a surface crust to restrict flow rates into the soil (Booltink et al., 1991). By offering slight hydraulic resistance to water movement, discs and crusts allow a water supply potential h to be applied at the soil surface, with a negligible head loss. By appropriately choosing the resistance value and ensuring that h is only -0.01 to -0.02 m, an acceptable approximation of soil hydraulic conductivity is obtained, which excludes the macropore system. It is thus possible, by the resolution of the 3-dimensional moisture flow field, to obtain soil hydraulic properties for water content values near saturation.

Finally, it is worth mentioning particular calculation methods proposed in the literature and set up for estimating hydraulic conductivity from disk permeameter data. Among others, the most commonly used are those proposed by White and Sully (1987) and by Ankeny et al. (1991). Such methods vary in complexity and simplifying assumptions, as well as having different advantages and limitations.

3.4.1 Disk permeameter

The apparatuses used to impose Dirichletís boundary condition $h_0 \leq 0$ at the soil surface, in which ho is the water supply potential, are called tension infiltrometers or disk permeameters in the literature.

Following the design of Perroux and White (1988), a permeameter (Figure 22) was set up by the Hydrology laboratory of the Dept. DITEC, University of Basilicata, Italy. The permeameter in question consists of a bubble tower which may be considered a Mariotte double regulator connected to a perspex disc 200 mm in diameter covered by a porous nylon membrane with air entry value of approximately 0.25 m. The first regulator allows us to apply via the membrane a constant water supply potential which can be controlled by adjusting the water level inside. The second regulator, which functions as a reservoir by means of a graduated scale, allows infiltration water volumes to be evaluated in time.

The experimental observations which may be carried out with such a device necessitate, between the base of the disc and the soil surface, that there is adequate hydraulic contact by means of a thin sand stratum previously wetted up to a volumetric water content close to 0.01.

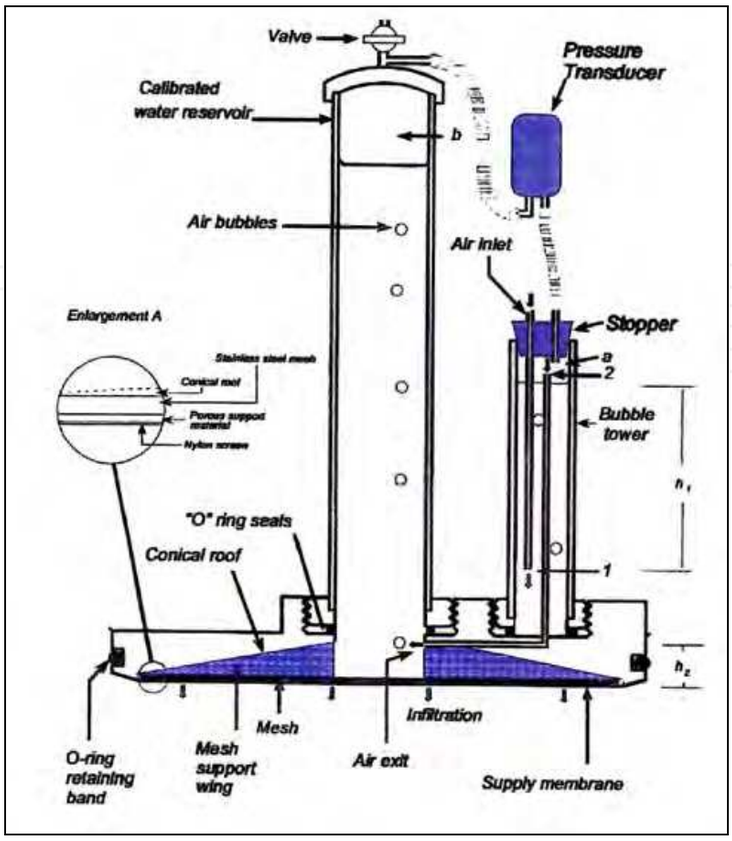

Fig. 22. Schematic illustration of the disk permeameter (Source:Evett et al., 1999)

3.4.2 Theory

The theoretical foundations for using a disk permeameter to infer soil hydraulic properties have been discussed in detail elsewhere (Perroux and White, 1988; Smettem and Clothier, 1988). Only the salient features are recalled below:

Sorptivity

The water flow emanating from a disk source according to Dirichlet boundary condition:

$h=h_0 \leq 0$; $z=0$; $t>0$

where h_0 is the water supply potential, z is the depth and t is the time, is initially controlled by soil capillarity (Philip, 1969):

$$\lim_{t\to 0}\left[\frac{Q(t)}{\pi r^2}\right]=\frac{1}{2}S_0 t^{-1/2} \tag{31}$$

in which Q is the flow rate ($L^3\ T^{-1}$) from the disc source, *t* the time, *r* the radius of the source (L), $S_0=S(h^0, h_n)$ the sorptivity ($LT^{-1/2}$,)and h_0 and h_n, respectively, the supply and initial water potential (L).

Integrating equation 31 with regard to *t*, we obtain:

$$I = S_0 t^{1/2} \tag{32}$$

in which I is the cumulated infiltration (L).

For lower time values starting from infiltrated water volumes, So may be simply deduced from the slope of I with regard to $\sqrt{t}$.

The geometric time scale of Philip (1969), t_{geom} may be used to evaluate when the geometric dominance of disc source should have been established.

This time is considered to be:

$$t_{geom} = \left[\frac{r\Delta\theta}{S} \right] \tag{33}$$

in which $\Delta\theta=\theta_0-\theta_n$ and θ_n are, respectively, water content values corresponding to the supply and initial water potential.

Steady state flow

The water flow rate will reach a stationary value henceforth termed Q_∞ for greater time values (Philip 1966).

In the case of multi-dimensional flow processes, Philip (1986) showed that a characteristic time scale t^* for the steady state flow rate is that for which the flow from the source is 1.05 times the steady flow rate. His calculations show that when the characteristic size of source r equals or exceeds the macroscopic capillary length scale, λ_c, an "innate soil length scale" as defined by Raats (1976), then it may be held that $t^*=t_{grav}$, with t_{grav} given by :

$$t_{grav} = \left(\frac{S}{k_0} \right)^2 \tag{34}$$

The above findings were recently confirmed by Warrick's studies (1992). Physically, t_{grav} represents the time in which the effects of gravity equal the effects of capillarity (Philip, 1969).

(Gardner, 1958) introduced the concept of "alpha" soils, that is soils whose hydraulic conductivity takes the exponential form $K = K_0 \exp(\alpha \mathrm{h})$, with α is a constant equivalent to λ_c^{-1} . In the case of "alpha" soils, Wooding (1988) showed that the steady flow from the source, for an assigned value of water supply potential, may be approximated with sufficient accuracy by the following expression:

$$\frac{Q_\infty}{\pi r^2} = \Delta K \left[1 + \frac{4\lambda_c}{\pi r} \right] \tag{35}$$

in which $\Delta K=K_0-K_n$.

Subsequently, White and Sully (1987) demonstrated that between the characteristic length scale k, sorptivity and hydraulic conductivity, there may be the following type of relation:

$$\lambda_c = \frac{bS^2}{\Delta\theta\Delta K} \tag{36}$$

in which b ($1/2 \le b < \pi/4$) is a shape factor frequently set at approximately 0.55 for agricultural soils.

If, as happens in many open field situations, it may be assumed that: $\Delta K = K_0 = K$ and if we substitute equation (36) in (35), the following simplified expression is obtained:

$$\frac{Q_\infty}{\pi r^2} = K + \frac{2.2S^2}{\Delta\theta\pi r} \tag{37}$$

An alternative approach based only on Wooding's solution is possible when we know the flows Q_∞ corresponding to the different *r* values of the source (Scotter et al., 1988, Smetten and Clothier, 1989). This approach allows K and λ_c to be evaluated directly, thereby solving two type (35) equations.

The same principle may be applied for a single r of the disc source but with infiltration measurements at multiple potentials (Ankeny, 1991). In particular, in this case, if the flow is measured with a single disc source at two pre-established potential values h_1 and h_2, two type (35) equations are obtained, which may be solved simultaneously, thereby supplying:

$$\begin{aligned} K_1 &= \frac{Q_1}{\pi r^2 + 2\Delta h r\left(1+\frac{Q_2}{Q_1}\right)\left(1-\frac{Q_2}{Q_1}\right)} \\ K_2 &= \frac{Q_2 K_1}{Q_1} \\ \lambda_c &= \frac{\Delta h\left(K_1+K_2\right)}{2\left(K_1-K_2\right)} \end{aligned} \tag{38}$$

in which Q_1, and Q_2 are, respectively, Q_∞ at h_1, and h_2.

3.4.3 A case study

Infiltration tests were conducted at the experimental farm of the University of Basilicata near Corleto (Potenza, Italy) on bare soil which had undergone minimum tillage during the winter. The dominant soil at the experimental site is sandy clay (sand 36.5%, silt 24.1%, clay 39.4%).

From the pedological point of view, the soil may be classified as. "vertic ustorthens" according to the USDA classification system. Other important properties comprise moderate permeability and the vertic traits of clayey land which cracking renders quite appreciable during the summer.

At the test location one (1x1 m^2) plot was isolated and subdivided into 4 equal subplots of 0.5x0.5 m^2. To determine soil hydraulic conductivity with White and Sully's method (1987), three water supply potential were used (-0.02;-0.06;-0.10 m), each in a single subplot.

According to the Ankeny et al. method (1991), in the 4th subplot the disc permeameter was not moved for trials at the three potentials (-0.06;.-0.04;-0.02 m). With this method, steady state flows were measured in an ascending sequence of supply potentials: first with a -0.06 m water supply potential followed by -0.04 and -0.02 m.

In each subplot, three undisturbed soil samples, 4.8 cm in diameter and 2.8 cm in height, were taken from the soil surface before and after the infiltration tests in order to measure bulk density and volumetric surface water content θ corresponding to h_0 and h_1. The mean dry bulk density of the first 2.8 cm of soil measured on undisturbed soil samples was estimated at 1.198 g/cm^3 and the standard deviation at 0.05 g/cm^3.

Following disk permeameter measurements, the soil was allowed to drain for about three hours and then an undisturbed soil sample 15 cm in diameter and 20 cm high was dug out of the 4th subplot immediately below the porous disk, to measure the hydraulic conductivity in the laboratory with the crust method (Figure 23)(Booltink et al., 1991; Coppola et al., 2000).

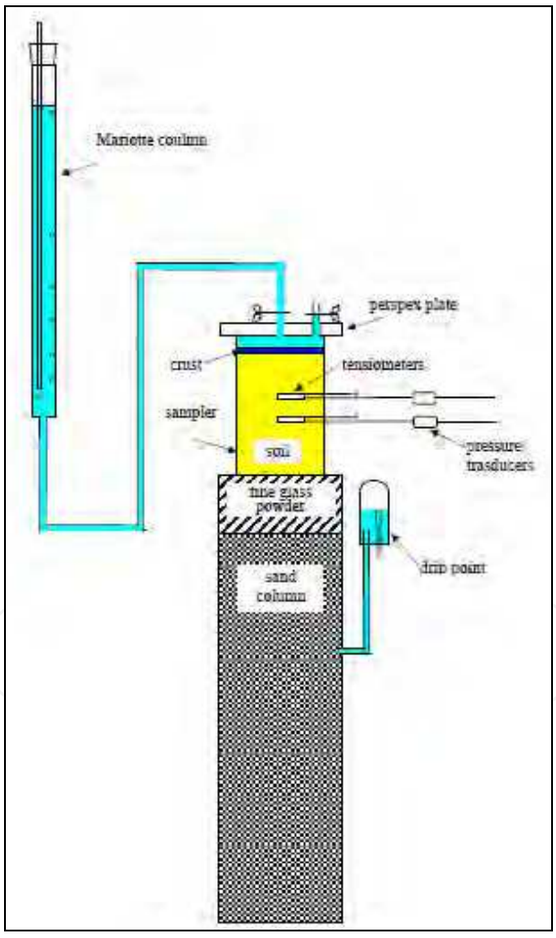

Fig. 23. Schematic illustration of the crust method apparatus

This method requires a pedestal of soil and a Stackman sand filter for draining the soil samples slowly saturated from the base. Conductivity values are determined during steady

vertically downward flow under unit hydraulic gradient measured with small tensiometers. Once it has been ascertained that the water flux density in is equal to the water flux density out, the hydraulic conductivity will be equal to the imposed water flux. Moreover, it is worth noting that under the condition of unit hydraulic head gradient the matric potential at different depths is uniform, the water content is fairly uniform and, consequently, the accuracy in the estimate of K will only depend on measurement errors. Thus, the function K(h) of the soil in question was deduced with great accuracy, applying a series of steady water flux densities for an extended period of time by means of a porous disk connected to a bubble tower to control the water supply potential in a field of variation between 0 and -0.20 m and evaluating the hydraulic gradient from the tensiometer measurements at depths of 0.025 and 0.075 m.

White and Sully (1987) calculate sorptivity by means of equation (32). By contrast, Q_∞ is estimated for greater time values and the same authors use equations (36) and (37) to calculate the hydraulic conductivity. Thus, in using equation (36) $\Delta\theta$ is still required.

The main theoretical assumption underpinning the method is that cumulative infiltration I for lower t values varies linearly with the square root of time and, for greater values, linearly with t. Figures 24(a) and 24(b) show that for the soil in question the features of flow theory for disc permeameters are satisfied. Indeed, the above Figures clearly show that for the 3 different water supply potentials, data quality is sufficient and that data are always widely available to determine So by regression of I against t at the straight line portion of Figure 24(b) for t values from 0 to roughly 100 s. On the other hand, Q_∞ may be evaluated by regression of $I(t)$ against t for the long straight portion of Figure 24(a).

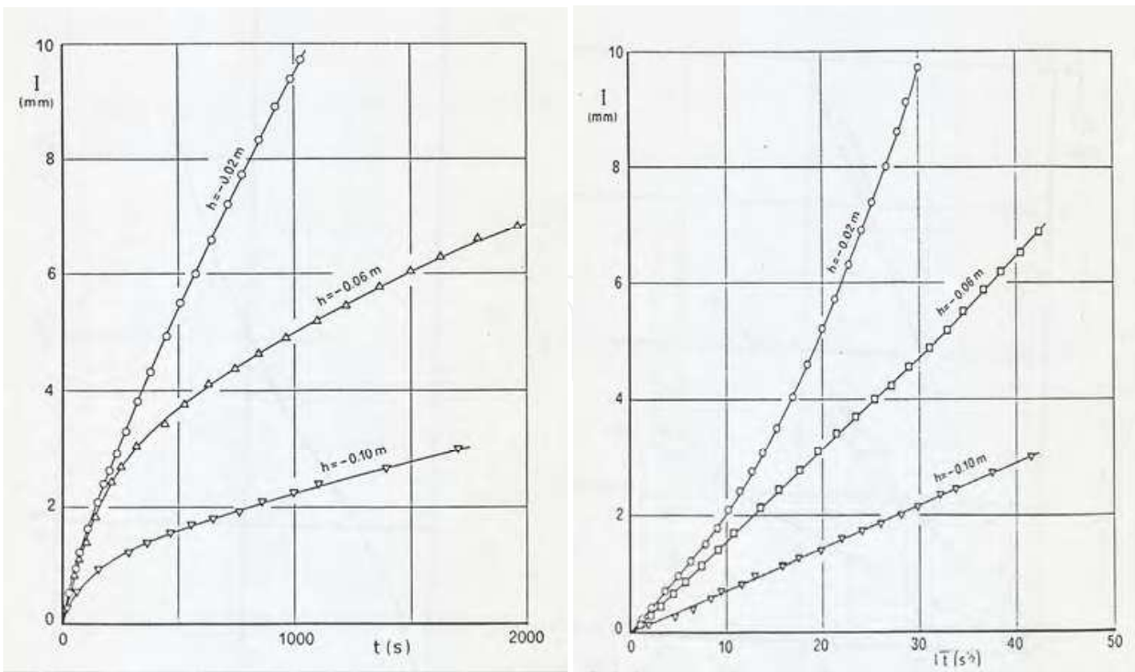

Fig. 24. a. In situ cumulative infiltration over time and b. over square root of time during 3D flow from disk permeameter for three water supply potentials

In the observed situation, it seems reasonable to expect a steady flow rate within less than an hour, which allows sufficient Q_∞ data to be obtained most rapidly. This last consideration is interesting in the case where it is intended to conduct inquiries to ascertain the level and pattern of spatial or temporal variability.

Amongst the methods based on Wooding's equation (35), the method proposed by Ankeny et al. (1991) is based only on measurements of steady-state flow rate Q_∞. However, determining when Q_∞ is reached may be very difficult (Warrick, 1992).

With regard to Figure 25, for the soil in question the mean time for reaching steady-state flow for the -0.06 m water potential was 100 s, followed by 400s to attain steady-state flow at -0.04 m water potential and finally 650 s for -0.02 water potential. In the above case, Q_∞ is obtained by the regression of $I(t)$ against t from Figure 25 and equations (38) are used to calculate conductivity K . Unlike the White and Sully method, in the Ankeny method measurements of θ_0 and θ_n are entirely avoided.

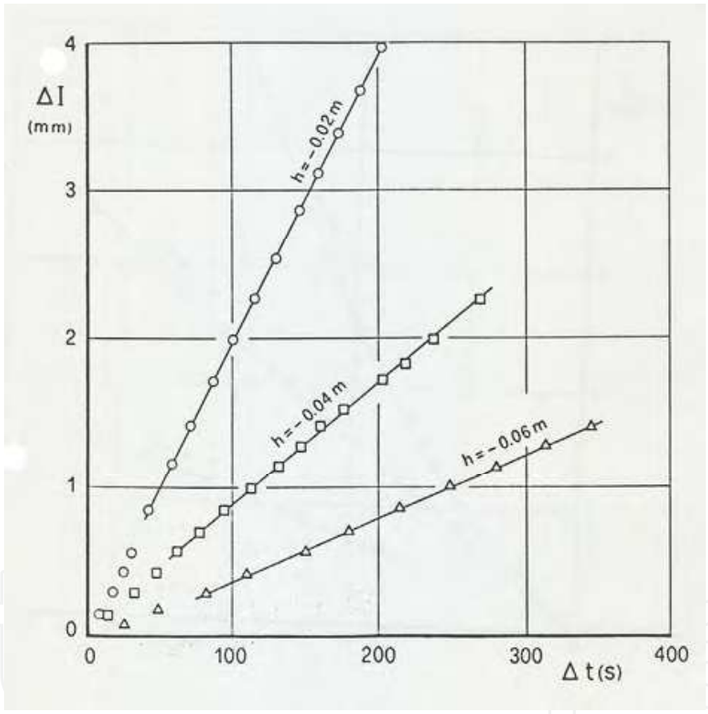

Fig. 25. Steady state flow intake for three water supply potentials

Conductivity values calculated by the various methods adopted are given in Figure 26, which also supplies, for the sake of comparison, laboratory core measurements of k based on the crust method. In particular, note that the K values calculated by the Ankeny method are in good agreement with the k values determined with the crust method. In any case, the bias ascertained for the White and Sully method to underestimate K values is within less than one order of magnitude.

The analysis of behaviour at the origin of function k(h) evidences a bimodal distribution of the porous system of the examined soil, with a water potential break-point at ≈-0.03 m. With

the increase in water potential from -0.02 m to 0, hydraulic conductivity increases by about an order of magnitude, nonetheless assuming numerical values greater than those measured in a previous measuring campaign on undisturbed soil samples taken in the same sites. Such behaviour suggests that the structural porosity of this clay soil may play a dominant role in determining the pattern of water flow in the field.

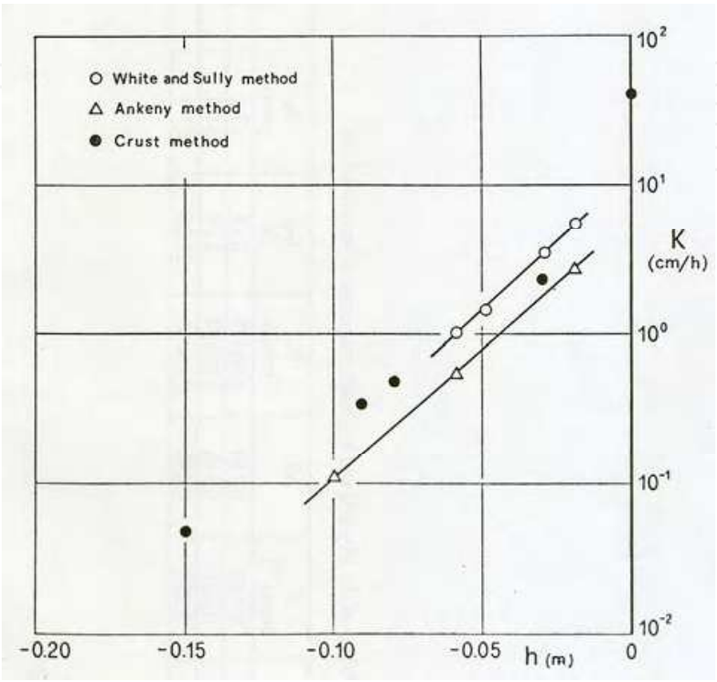

Fig. 26. Comparison of estimates of unsaturated hydraulic conductivity obtained using three different methods

Furthermore, to represent this bimodal pore system, a two-line regression model may be more responsive than the usual linear model, or than the model with several parameters proposed by van Genuchten (1980). Such findings were also reached by Messing and Jarvis (1993) in a similar pedological context.

Philip (1985), starting from macroscopic capillary length λ_c, infers a representative pore size λ_m (mm) by using the capillary theory:

$$\lambda_m = \frac{\tau}{\rho g \lambda_c} \cong \frac{7.4}{\lambda_c} \tag{39}$$

in which τ and ρ are, respectively, the surface tension and the water density, and g is the acceleration of gravity. The characteristic size λ_m defined by White and Sully (1987) to be a "physically plausible flow weighted pore size" may be considered a representative index of soil structure.

Starting from the measured values of S_0, K and $\Delta\theta$, estimates were made by means of equation (9) of λ_m, values which are supplied in table 4 together with the values of λ_c and t_{grav}.

h (m)	S (mm/s$^{1/2}$)	Δθ	K (mm/s)	t_{grav} (h)	λ_c (mm)	λ_m (μm)
-0.020	0.193	0. 80	0.00697	0.17	13.1	572
-0.060	0.161	0.146	0.00154	3.04	64.4	118
-0.100	0.095	0.090	0.00035	21.20	122.6	61

Table 4. Values of physical and hydraulic properties of the examined soil

Examination of the table shows that the bimodal distribution is clearly evidenced by λ_m which shows a 9-fold change between -0.02 and -0.1 m water potential compared with a 5-fold change between -0.02 and -0.06 water potential and only a 2-fold change between -0.06 and -0.1 m water potential. At h>-0.06 m the influence of capillarity is very strong and t_{grav} is large. However, macropore flow increases as h approaches 0 and thus gravity flow is dominant at h<-0.06 m.

4. Spatial variability of soil physical properties

In light of the above, it appears evident that by improving measurement techniques and setting up mathematical models water flow in soil can be quantitatively determined. Moreover, since the transport in soils of solutes, pesticides and urban and industrial waste products, besides the reaction kinetics, is strictly linked to conductivity and hydraulic gradients, obviously only through knowledge of hydraulic characteristics is it possible to set up mathematical models that describe the environmental problems connected with such transport.

The results obtained from model applications depend on the quality of input data which, for field determinations, are greatly affected by the spatial variability of soils (Beckett and Webster, 1971). Soils vary considerably from place to place and only with accurate measurements can such variability be described. With pedological studies, soils can be classified and mapped, usually performed with a view to serving many applications and based on various factors, of which hydraulic properties play a minor role.

The various cartographic units have mean values with variations that are considered negligible, and depend on the classification scheme adopted and the scale of representation. Hence within the various cartographic units there are variations in hydraulic properties that cannot always be ignored. Applications of models to field conditions may lead to unacceptable errors when we consider soil as a homogeneous medium and, even more, when variations along the profile are considered, identifying layers in various horizons, each of which has mean values of functions $K(\theta)$ and $\theta(h)$. Thus soil has to be considered as a medium in which the properties are tied to spatial coordinates and, in the event of anisotropy, to direction.

Bearing in mind that soil extends over a large area in relation to its thickness and in the case of isotropy, hydraulic properties should always be considered, for each horizon, a function of two coordinates. A deterministic definition of spatial heterogeneity requires a large number of measurements and hence, owing to the burdensome, highly costly nature resulting from the complexity of testing techniques, cannot be pursued except for problems that affect limited zones. Moreover, flow processes should be viewed as three-dimensional, and their modelling would require high calculation costs with the use of computers with large memory capacities and high speeds, which are not always readily available.

Hence spatial variations in soil hydraulic properties are to be considered irregular, determined by innumerable parameters according to complex imperfectly known laws, which is why they appear essentially random and hence can be described only by means of statistical procedures. Working on an area of 150 ha, homogeneous in pedological terms, Nielsen et al. (1973) were the first to determine, at 20 randomly chosen sites and at six depths, the hydraulic conductivity curves $K(\theta)$ and those of tension $\theta(h)$, together with other physical parameters of the soil. The data show considerable variability from zone to zone and allowed, for each quantity measured, the corresponding frequency distribution to be identified.

The avenue pursued by Nielsen was then followed by others (Coelho, 1974; Carvallo et al., 1976; Kutilek and Nielsen, 1994; Coppola et al., 2009), who carried out surveys to characterise the heterogeneity of areas of different size. The data show marked variability also with reference to fairly small areas, especially as regards hydraulic conductivity and diffusivity which show variation coefficients in excess of 100%.

4.1 Simultaneous scaling analysis of soil water retention and hydraulic conductivity curves

The description of the spatial variability of hydraulic parameters may also be simplified by hypothesizing that soil microgeometry in two different sites is similar. As shown by Miller and Miller (1955a, b), values of water potential and conductivity measured in different zones may be related to corresponding averages through spatial distribution of the local similarity ratio *a*.

The validity of this hypothesis has been confirmed only through laboratory tests on sand filters (Klute and Wilkinson, 1958; Elrick et al., 1959) and, even if it finds no actual correspondence in soils, it has been used by several authors (Warrick et al., 1977b; Simmons et al., 1979; Rao et al., 1983) to relate potential and conductivity to the degree of soil saturation s and not to water content θ. The same authors evaluated the distribution of the similarity ratio not with reference to the microgeometry of the porous medium, but by ensuring that there was the best possible fit between the tension and conductivity curves, measured at various points.

Thus the rigorous concept of geometric similarity introduced 30 years ago by Miller and Miller is superseded and the similarity ratio is determined using regression techniques. The purpose of such techniques, generally indicated in the literature as being *functional normalization* (Tillotson and Nielsen, 1984), is to reduce dispersion of test data, concentrating them on an average reference curve that describes the relationship in question. Scale factors α identified with such procedures often differ in each hydraulic property on which they are evaluated (Warrick et al., 1977b; Russo and Bresler, 1980; Ahuja et al., 1984).

Application of the similarity concept to the water budget of a small river basin or an irrigation area has recently proved promising (Peck et al., 1977; Sharma and Luxmoore,1979; Warrick e Amoozegar-Fard, 1979; Bresler et al., 1979). Using a simulation model, the latter authors examined the effects of spatial variability of soil hydraulic properties, expressed in terms of each stochastic variable α, upon the components of the water budget. The various components of the budget, simulated by attributing log-normal frequency distributions to a,

are in excellent agreement with the experimentally measured values. The literature also indicates that field-scale tests to apply the similarity concept are still too few and in any case restricted to soils with reasonably similar morphology.

4.1.1 Theory

In order to reduce dispersion of the experimental data and define a single average curve both for function h(s) and for k(s), the above-cited similarity theory expounded by Miller and Miller was applied. *The latter showed that, assuming constant* surface tension and the kinematic viscosity coefficient of water, for two porous media with geometric similarity the following formula holds:

$$W_r = \alpha_{w,r}^{p} \overline{W} \tag{40}$$

which links a generic hydraulic property W_r , determined in a site r, to the value $\overline{W}$ of the reference site. Factor $\alpha_{w,r}$ is the relationship between the lengths of the inner geometry of the medium at site r and those of the reference medium, while exponent *p* assumes the value -1, when the hydraulic property in question is the water potential h, and 2 when reference is made to hydraulic conductivity K. Under the similarity hypothesis the $\alpha_{w,r}$ coefficients are the same for any hydraulic property and the two sites have the same value of porosity. The values of coefficients a were determined for the area in question, expressing for each site *r* the relations linking the water potential h and hydraulic conductivity k at saturation s by means of assigned analytical functions.

It was postulated that one of the parameters appearing in the analytical relations, namely *ar*, depends on the measurement site, while the remaining ones, numbering m, assume the same values throughout the zone in question. Hence the following expression was used:

$$W_r = a_r f_w\left(s; b_1, ..., b_m\right) \ \left(r = 1, ..., n\right) \tag{41}$$

where *n* indicates the number of sites taken into consideration.

Having assigned the analytical expression for f, the parameters in question were determined by minimising the sum M of the square deviations between the values of the hydraulic property W, determined by function f_w, and the corresponding measured values $W_{r,j}$.

Hence to determine M the following expression was used:

$$M = \sum_{r=1}^{n} \sum_{j=1}^{n_r} \left[a_r f_w\left(s_r, j; b_1, ..., b_m\right) - w_{r,j} \right]^2 \tag{42}$$

in which n_r is the number of points of curve W(s) relative to site *r*. Since the function f_w is generally non-linear, the minimum of M was sought with an iterative method similar to that proposed by Simmons et al. (1979) and a calculation program was specially written which, enabled rapid determinations starting from an initial estimate of parameters quite far from the solution.

Finally, the coefficients $\alpha_{w,r}$ defined by equation (40) were obtained by imposing the normalization condition:

$$\frac{1}{n}\sum_{1}^{n}\alpha_{w,r}=1 \tag{43}$$

4.1.2 A case study

The present section aims to ascertain the validity of the method in context. In the following, we will provide some results of the case study illustrated in the section 3.1.1. For all the samples analyzed in Figure 27, in the function of degree of saturation, s, the values of potential $\bar{h}=\alpha_{h,r}h$, are presented, while in Figure 28 the conductivity values $\bar{k}=\alpha_{k,r}^{-2}k$ are given, obtained by processing the potential and conductivity data respectively.

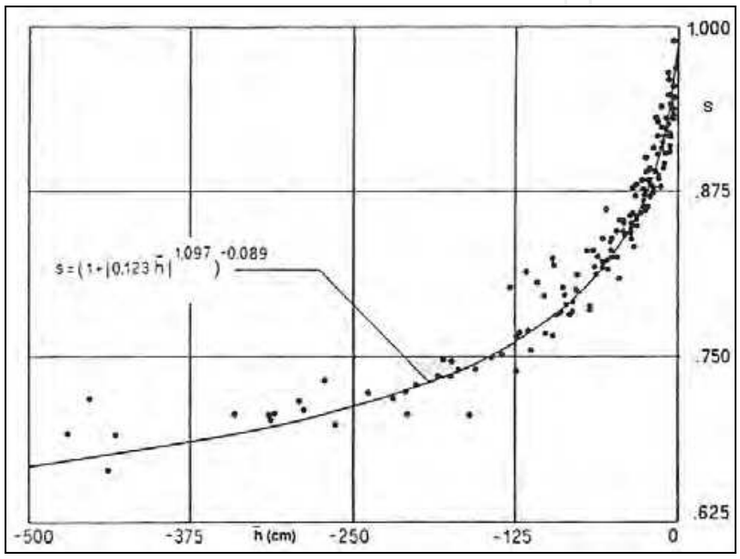

Fig. 27. Scaled soil water retention data for the composite

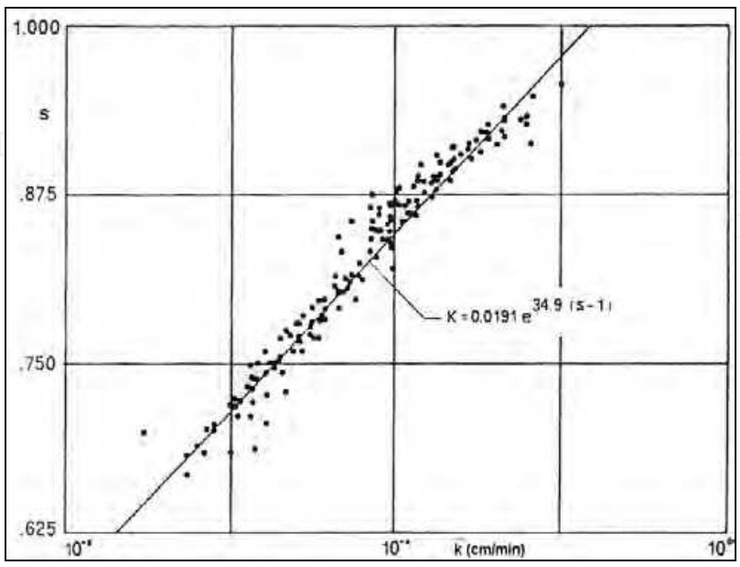

Fig. 28. Scaled hydraulic conductivity data for the composite

The graphs show how the method we adopted markedly reduces the dispersion of experimental points and allows the evaluation of the variability of the hydraulic properties of soil through the spatial distribution of the sole parameters $\alpha_{h,r}$ and $\alpha_{K,r}$.

The statistical processing thus demonstrated how the log-normal rule is that which best approximates to frequency distribution, not only to the parameters $\alpha_{h,r}$ but also to those $\alpha_{K,r}$. The principal statistical moments of $\alpha_{h,r}$ and $\alpha_{K,r}$ are given for the applications in table 5.

	$A_{h,r}$	$\alpha_{K,r}$
mean	0.978	1.098
standard error	0.924	1.968
CV	0.945	1.793

Table 5. Values of mean, standard deviation and coefficient of variation of the scale factors determined respectively from h(s) and K(s) data

A study of the table reveals that the coefficients of variation obtained by processing the conductivity data are higher than those relative to the processing of the potential data, which is probably due to the fact that conductivity values are more sensitive to degrees of saturation. It must, finally, be underlined that the high degree of correlation between parameters $\alpha_{h,r}$ and $\alpha_{K,r}$ supports the macroscopic similarity hypothesis of Miller and Miller (1955).

4.2 Geostatistical analysis

A survey of the recent literature shows that various techniques are adopted to determine the spatial variability structure of soil hydraulic prperties. The possible periodicity of data may be highlighted through the spectral density function determined by adopting smoothing techniques to remove any errors to remove any errors (Webster, 1977). Under the assumption that soil parameters may be represented by random stationary functions, with finite mean and variance, the autocorrelation function can be defined as dependent only on the distance between observation pairs. The diagram of the autocorrelation function then allows us to determine up to what distance the observations are correlated with one another (Vauclin et al., 1982; Webster and Cuanalo de la C., 1975).

Recently, geostatistical techniques developed originally by Matheron for mining estimates (David, 1977; Journel and Huijbregts, 1978) have been profitably used to study the spatial variability of soil physical and hydraulic properties.

4.2.1 Theory

Like natural phenomena which, over space or time, show a structure and in geostatistics are termed regional phenomena (Matheron, 1971), by the same token hydraulic parameters may be considered regionalized variables. Indeed, with the use of stochastic procedures developed in the context of geostatistics, soil hydraulic parameters, actually functions with values distributed in space, come to be represented as stochastic variables Z, with discrete values assigned according to probability distributions laws.

At each point the properties of Z thus remain defined through the mean value, variance and covariance, with means referring to the ensemble of realizations at the point considered.

For practical purposes, it is nonetheless necessary to make some simplifying assumptions, since the probability distribution functions at each point in space are not known, nor can they be deduced in the availability of a single realization of the parameter in question.

Reference is therefore made to the intrinsic hypothesis and the stochastic variable is assumed to remain defined through a single function at all points. In relation to increases in Z, $Z\left(x+\bar{h}\right)-Z(x)$, for the assumed stationary conditions, there is a zero mean and variance independent of x. Moreover, in the availability of observations concerning distinct points being considered a single realization in space, with reference to the ergodic hypothesis it is assumed that the mean values obtained on the ensemble realizations for the single points may refer to spatial mean. Under such hypotheses, the variogram function remains definite:

$$\gamma(h)=\frac{1}{2}E\left[\left\{Z\left(x+\bar{h}\right)-Z(x)\right\}^2\right] \tag{44}$$

and again for the covariance, C(h), and variogram, $\gamma\left(\bar{h}\right)$, functions only of vector $\bar{h}$,usually known as lag, the following condition is satisfied:

$$\gamma\left(\bar{h}\right)=C(0)-C\left(\bar{h}\right) \tag{45}$$

in which C(0) is none other than the variance of the process Z(x) assumed stationary and ergodic.

Upon verification of such hypotheses, the variogram function describes the structure of a regional variable of known value in a discrete number of points mostly distributed irregularly. Complete interpretation of the variogram function may be found in Journel and Huijbregts (1978). However, in short, with reference to a typical semivariogram, it may be stated that in the cases in which γ(h) is constant upon the variation in h, the values of the parameter in question may be considered spatially uncorrelated.

When, as h increases, γ(h) grows towards a constant value $C_1+C_0=C$, the observations are correlated amongst themselves as far as a distance h_0 at which the variogram may be held to have reached C. The maximum value C of the variogram is indicated as the sill and typically supplies an estimate of variance, while the distance h_0 at which γ(h) first reaches the sill value is indicated as a range. In theory, for h=0 we should have γ(0)=0, but the extrapolated test variograms that make h tend to zero are approximated to a value C_0 different from zero, called nugget effect which is indicative of the variability of the parameter at a smaller scale than the minimum sampling distance and the random errors tied to the measuring techniques used.

Once the spatial dependence of the observations has been identified, geostatistical techniques allow the burden of measurements to be contained by determining the minimum number of measurements, the optimal distance and their location. Moreover, with knowledge of the variogram function it is possible to apply optimal interpolation techniques (kriging) which allow fairly detailed spatial distribution maps of the various parameters to be drawn with a smaller number of observations (Burgess and Webster, 1980).

4.2.2 A case study

To show the presence of a spatial structure of the soil hydraulic properties, below we will analyze data coming from the experiment illustrated in section 3.2.2. To express the law of retention θ(h) we adopted the analytical relation proposed by van Genuchten (1980):

$$\theta(h) = \theta_r + \frac{\theta_s - \theta_r}{\left[1 + (\alpha|h|)^n\right]^m} \tag{46}$$

in which α and n are essentially empirical parameters, θ_s is the value that θ assumes at saturation, and θ_r represents residual water content, that is, what is found for h tending to minus infinity.

For the conductivity curve the exponential relation (Libardi at al, 1980) was used:

$$K(\theta) = K_0 \exp\left[\beta(\theta - \theta_s)\right] \tag{47}$$

in which β is an empirical parameter and k_0 represents the value of hydraulic conductivity for $\theta=\theta_s$.

Of the parameters which feature in relations (46) and (47), θ_s was determined with sufficient accuracy by means of measurements made at the end of the infiltration process, while θ_r was set at zero. Soil hydraulic properties are thus defined by the values of only four parameters: α, n, K_0 and β.

Table 6 gives a synopsis of results of all the determinations using exploratory statistics: mean, standard deviation and coefficient of variation. The physical properties of the soil in

		Statistical indices		
		μ	σ	CV (%)
Physical properties:	Sand (%)	80.0	3.84	4.80
	Silt (%)	12.0	0.68	5.67
	Clay (%)	8.0	0.26	2.06
	ρ_b (g/cm³)	1.16	0.05	4.31
Hydraulic properties:	θ_s (-)	0.526	0.047	9.1
	θ_{-100} (-)	0.419	0.041	9.79
	θ_{-200} (-)	0.346	0.043	12.4
	θ_{-300} (-)	0.301	0.046	15.3
	Ks (cm/h)	8.31	3.75	45.13
	$K_{0.4}$ (cm/h)	0.051	0.031	60.78
	$K_{0.3}$ (cm/h)	0.0025	0.0018	72.00
	$K_{0.2}$ (cm/h)	0.00013	0.0001	76.92
Parametric curve coefficients	α (cm^{-1})	0.01	0.0026	26.00
	n (-)	1.46	0.139	9.52
	β (-)	29.9	5.56	18.60
	K_0 (cm/h)	0.50	0.48	96.0

Table 6. Exploratory statistics for some physical and hydraulic properties and parametric curve coefficients

question present a modest dispersion against the mean, with coefficients of variation on average equal to 4.21%. Also the coefficients of variation of water contents θ, for h=0, -100, -200 and -300 respectively, are somewhat low and on average equal to 11.6%. Moreover, as with the findings reported by Nielsen et al. (1973), the hydraulic conductivity values experience considerable variability with a coefficient of variation exceeding 60%. Finally, on examining the data for the four parameters represented in equations (46) and (47), the distributions of values α and β present dispersion around the mean greater than that of n, while the coefficient of variation of K_0 is 96%, higher than that observed for the conductivity K_s measured experimentally in the field.

Comments on the data in table 6 implicitly assume that the observations of the physical and hydraulic properties of the soil in question are independent of the point at which they were made. In reality, each property is never distributed in a disordered way: a certain spatial structure is always present.

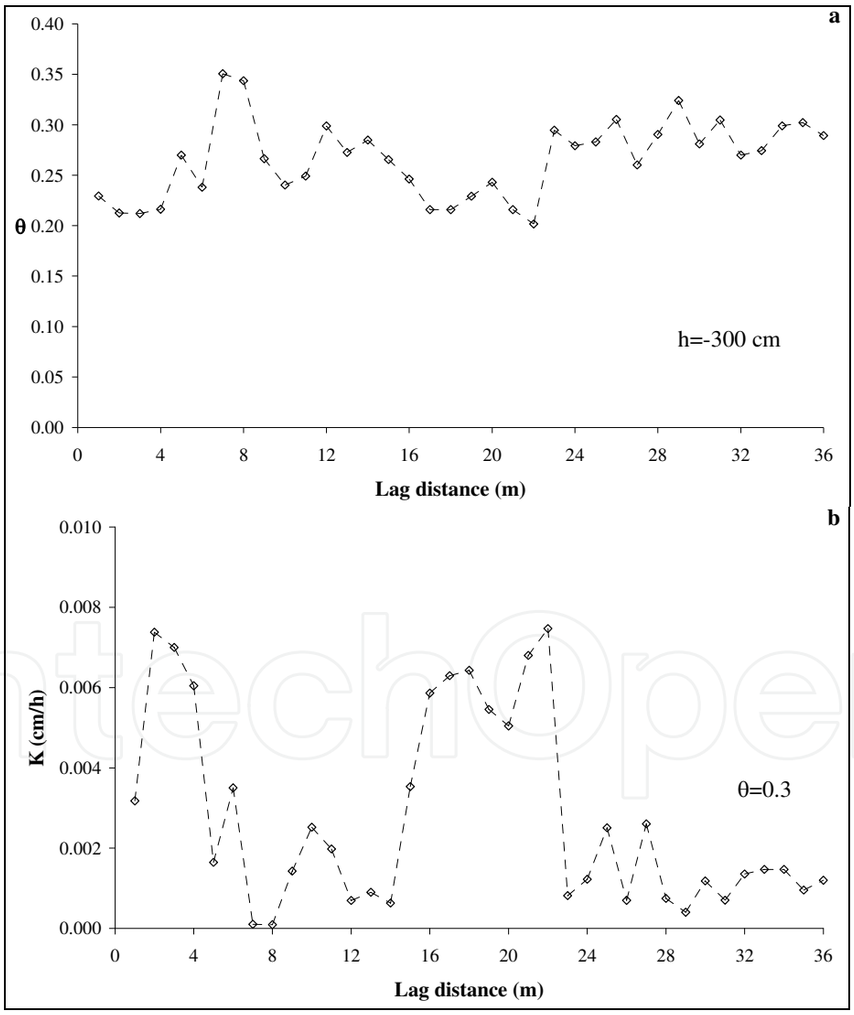

Fig. 29. a. Series of θ_i values, i=1, 2,…36 obtained from water content measurement for h=-300 cm; b. Series of K_i values, i=1, 2,…36 obtained from estimation of hydraulic conductivity for θ=0.300

To show the presence of a spatial structure for hydraulic properties of the soil in question, below in Figure 29a, b we provide spatial distributions of water content and hydraulic conductivity for the individual soil profiles along the transect at a respective depth of z=30 cm and z=45 cm.

It is inferred that θand K values show a discrete variability along the transects definitely tied to the local characteristics of the porous medium with deviation from the mean heavily dependent on the measuring point. The structure of spatial variability was then quantitatively evaluated using geostatistical techniques. The values of the experimental semivariograms γ for the data in Figure 29a, b are reported respectively in Figures 30a and 30b as a function of Lag, in other words the number of intervals between observations. The diagrams clearly show the presence of a spatial structure with values related between them up to a distance of about 7-9 m. Moreover, on fitting the diagrams for h=0, one notes that $\gamma(0) \neq 0$. This pattern that is often encountered in applications denotes the presence of noise components in the random function that may, in this case, be explained by random fluctuations, measurements errors and scale effects.

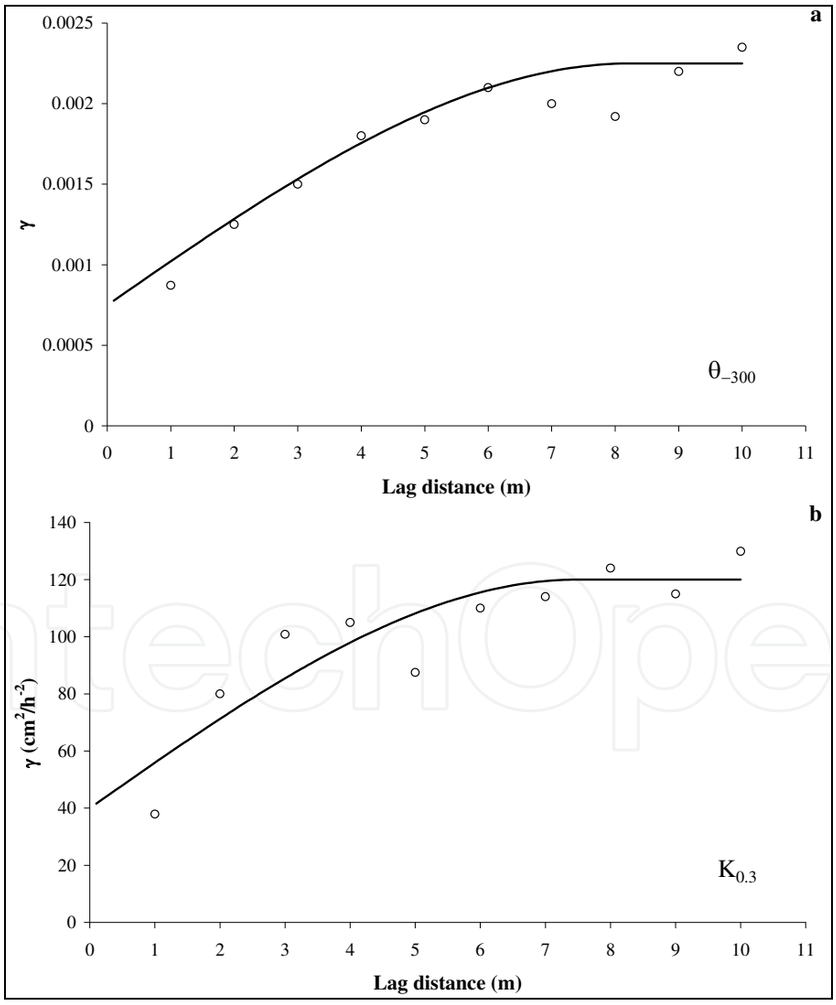

Fig. 30. a. Variogram relative to water content in Figure 29a; b. Variogram relative to conductivity in Figure 29b

The spherical model, chosen among the so-called authorised models, was then used to describe the variograms in Figure 30a, b. The iterative estimates, obtained with the least squares method from the model parameters, supplied the results of table 7. The last column of the table shows that 67% and 33% of the variability of θ and K is spatially structured.

Parameter	Field (m)	C_0	C_1	$100*C_1/(C_0+C_1)$
θ_{-300}	8.25	0.00075	0.0015	66.7
$K_{0.3}$	7.50	40	80	33.3

Table 7. Parameter estimation of the spherical model used for variograms of Figure 30a,b

4.3 State-space analysis

Another group of techniques, also used to study the structure of variability, is based on a modified time series theory (Box and Jenkins 1970). By using such techniques, the structure may be described in terms of autocorrelation functions and SARMA (Spatial Autoregressive-Moving Average) models with a view to estimating the stochastic properties of the data. Some of these applications in soil physics and hydrology include the studies by Morkoc et al., (1985); Anderson and Cassel, (1986); Wendroth et al., (1992); Cassel et al., (2000); Heuvelink and Webster (2001), Wendroth et all. (2006).

4.3.1 State-space model formulation

Clearly, there is a strict analogy between space and time, at least in the case of one-dimensional space. Hence, under the hypothesis of isotropy, analytical methods are to a broad extent equivalent. Typically, time series analysis allows us to analyse spatial structure in terms of autocorrelation functions and generalisation of state-space models. For this particular method of regression in the time and space domain, unlike the methods of kriging and cokriging (Vieira et al., 1983) the assumption of stationarity of observations is not required. The state-space method (Kalman, 1960) is particularly interesting when the phenomenon in question satisfies certain systems of differential equations. The method has been used in economics (Shumway and Stoffer; 2000) and has yielded good results in agronomic and soil science (Vieira et al., 1983; Morkoc et al., 1985; Wendroth et al., 1992; Comegna and Vitale, 1993; Wu et al., 1997; Cassel et al., 2000; Poulsen et al., 2003; Nielsen and Wendroth, 2003)

Let us use $Y(x)$, $x=x_o+1, ..., x_o+n$, to indicate the values assumed by n observations made for a certain soil parameter Y along a given transect (below we shall use the simpler notation Y_t, $t=1, 2, ..., n$). A state-space model consists, in the formulation most useful for our purposes (for details and generalisations see Anderson and Moore, 1979), of two equations:

$$\begin{cases} Y_t = F_t' Z_t + v_t \\ Z_t = G_t Z_{t-1} + w_t \end{cases} \Rightarrow \begin{matrix} Z_t = G_{1t} Z_{t-1} + G_{2t} Z_{t+1} + w_t \\ t = 1, 2, \ldots n \end{matrix} \qquad (48)$$

isotropic *anisotropic*

The first termed that of observations and the second that of transition, where F_t is a known vector (p, 1), Z_t is a vector (p,1) of the system state, G_t, G_{1t}, G_{2t} are a set matrices (p, p);

v_t~N(0; $\sigma^2_{v_t}$) independent of w_t~Np(**0**; Σ_{w_t}). The model (48) is wholly specified by the parameters (F_t, G_{it}, $\sigma^2_{v_t}$, Σ_{w_t}) and includes, as particular cases, other statistical models such as regression, ARIMA and SARMA models.

Having set the initial values, we may obtain optimal forecasts and estimates of the non-observable components by using the *Kalman filter*. At the same time, from many observations made of soil physical and hydraulic properties, the latter may plausibly have been generated by stationary *isotropic processes* with parameters independent of the individual measuring points:

$$E(Y_t)=\mu; \qquad var(Y_t)=\sigma^2 \qquad cov(Y_t,Y_{t\pm h})=c(h)$$

Hence we may consider the case in which the equations in (48) are reduced to simple ARMA and SARMA models. The importance of being able to make the double representation (state-space and SARMA or ARMA) lies in the fact that ARMA and SARMA models are easy to identify and estimate, while state-space models allow a more straightforward, immediate interpretation of the phenomena to which they are applied. Indeed, from (48) it follows that Y_t may be interpreted as the result of signal $F_t' Z_t$ which is overlaid by a random error v_t. Evolution of many physical phenomena can be well represented with a logical scheme like that reported in Figure 31.

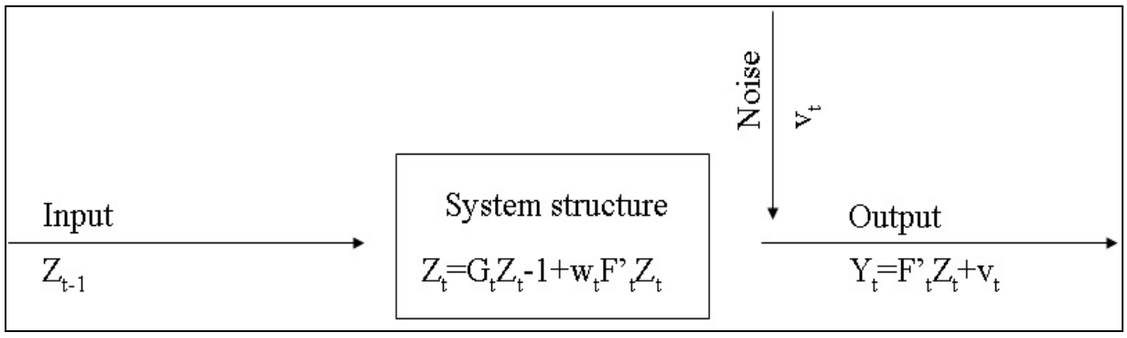

Fig. 31. Stochastic representation of input-output transformation model

The system structure is usually very straightforward and can be approximated, in the isotropic case, by an AR(1), given by:

$$Z_t = \phi Z_{t-1} + w_t$$

or, in the anisotropic case, a SAR(1) given by:

$$Z_t = c_0 + \phi_1 Z_{t-1} + \phi_2 Z_{t+1} + w_t$$

Note that, if it is $\phi_1 = \phi_2$ then the SAR(1) model may be replaced by the simpler AR(1) model.

Moreover, if we assume $p=1$, $F_t = 1$, $G_t=\phi$ then we obtain more simply:

$$\begin{cases} Y_t = Z_t + v_t \\ Z_t = \phi Z_{t-1} + w_t \end{cases} \Leftrightarrow \begin{cases} (-\phi B)Y_t = (-\alpha B)e_t \\ (1-\phi B)Z_t = w_t \end{cases}, \qquad t = 1,2,...,n \tag{49}$$

where B is the backshift autoregressive operator, $\phi_i > \alpha_i$ and e_t such that $e_t - \alpha_1 e_{t-1} - \alpha_2 e_{t-1} = v - \phi_1 v_{t-1} - \phi_2 v_{t+1} + w_t$. Thus both the equation of the observations and that of transition (i.e. the signal) are reduced to simple ARMA models and especially to an ARMA (1,1) for Y_t and an AR(1) for Z_t.

4.3.2 A univariate case study

In this section, we will still refer to the data set coming from the experiment shown in section 3.2.2, by analyzing individually the two parameters which characterize the soil water status in terms of θ and h measured at 0.3 m depth, along the N-S line of the plot so as to highlight their intrinsic structure linked to regional variability and, for 3 of the 12 measuring sampling times (the 3rd, 6th and 11th carried out 48, 168 and 768 hours respectively from the start of the drainage), the variations occurring in time (the parameters concerned are indicated by θ_i and h_i).

The data were first elaborated using classical statistical techniques, hypothesizing that the parameters vary in an essentially random manner. From this point of view, the main statistical indices (min. value, max. value, mean, standard deviation, skewness, kurtosis, coefficient of variation) of the above parameters are reported in table 8.

	Min	*Max*	*Mean*	*SD*	*Skew*	*Kurt*	*CV*
θ_3 (-)	0.307	0.383	0.341	0.019	0.217	-0.675	0.056
θ_6 (-)	0.257	0.330	0.287	0.018	4.462	-0.505	0.062
θ_{11} (-)	0.205	0.283	0.239	0.016	0.256	-0.353	0.068
θ_{100} (-)	0.236	0.300	0.257	0.015	0.655	-0.233	0.057
h_3 (cm)	58.0	103.1	83.2	10.4	-0.411	-0.217	0.125
h_6 (cm)	113.1	180.9	147.3	16.4	0.141	-0.700	0.111
h_{11} (cm)	189.7	305.2	244.9	27.8	0.108	-0.670	0.113

Table 8. Main statistical indices of the analysed series

From table 8 we may deduce, for all the measuring times considered, an increase in the standard deviation (SD) with its mean for parameter h, whereas the SD of θ is practically constant. We also note that the coefficient of variation (CV) of h is almost twice that of θ. Concluding, the two processes describing h and θ are, in time, both non-stationary on the mean, while h is also non-stationary in variance. Figure 32 illustrates the above points: it reports the 50 observations of θ and h for 10 of the 12 sampling times (from the 2nd to the 11th). This all agrees with the theoretical results obtained by Yeh et al. (1985), which predicted such behaviour on the basis of the stochastic analysis of unsaturated flow through heterogeneous media.

In the context of stochastic analysis it is essential to verify, for the parameters considered, the existence of a correlation structure.

Variables θ and h, given that they are recorded at constant intervals along the transect, are ordered in space and their evolution in the prefixed direction can therefore be evaluated by means of typical statistical analyses of the time series and in particular by means of the ARMA model (see Box and Jenkins, 1970) only when the hypothesis of isotropy can be

justified. A preliminary test was than carried out on θ_3 and h_3 series. The model which supplied the most acceptable results in terms of simplicity and interpretability, both because of the limited number of parameters and goodness of fit of the data, was SAR(1) model where the unknown parameters to be estimated are ϕ_1 and ϕ_2. The above criteria of choice was followed for all models subsequently used. It should be noted that if ϕ_1 and ϕ_2 are substantially equal than θ_3 and h_3 are to be considered isotropic, conversely anisotropy may be taken into account.

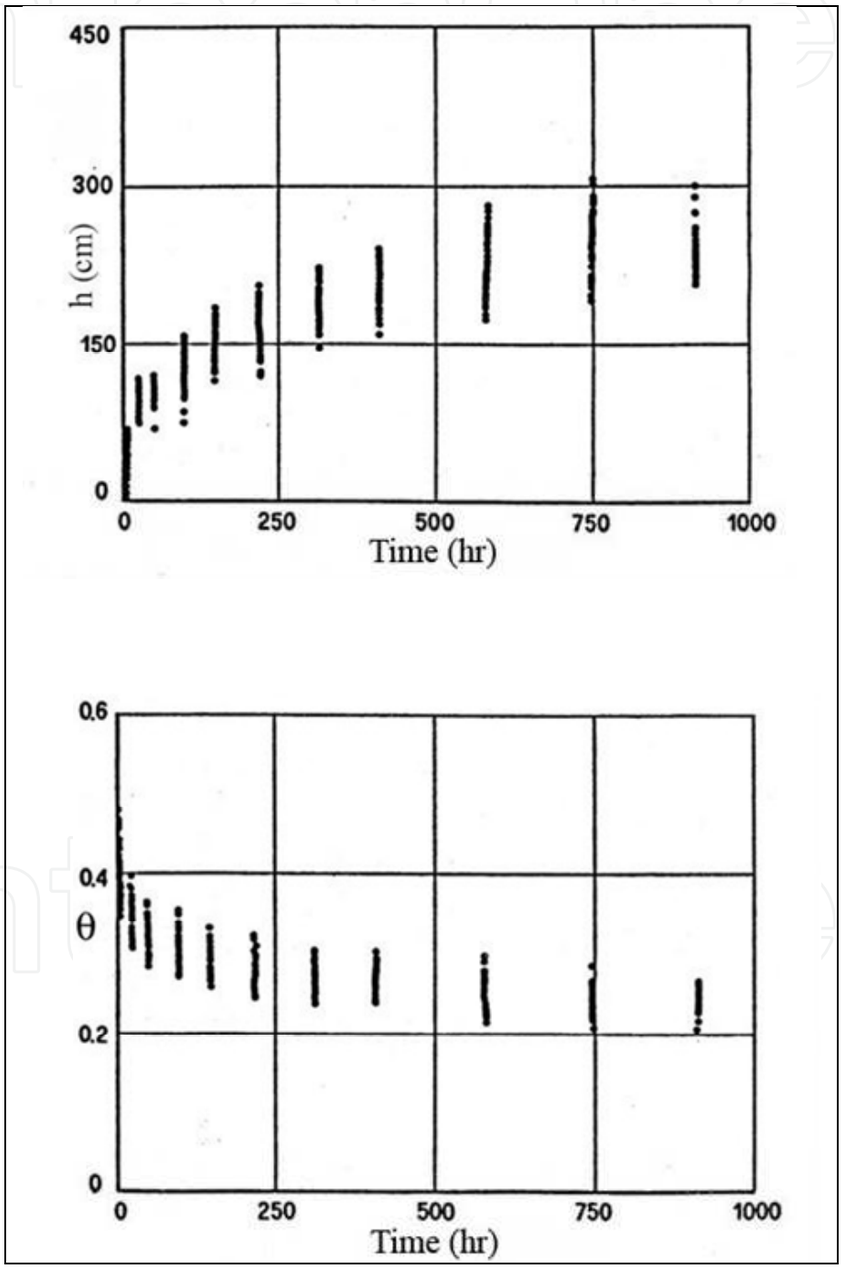

Fig. 32. Soil water potential h and volumetric water content θ as a function of time at the 0.3 m depth for all redistribution times during the drainage period

The iterative least-squares method estimate of the model parameters in question, provided the results reported in table 9 where standard deviations are in brackets. Having supposed that the phenomenon is isotropic and therefore invertible in space, the estimated ϕ_1 and ϕ_2 values are expected to be equal. In particular, in our case, we may observe that $\phi_1=\phi_2$.

	θ_3	h_3
c_0	0.0858 (0.0418)	29688.27 (12629)
ϕ_1	0.3950 (0.1409)	0.331 (0.1341)
ϕ_2	0.3530 (0.1488)	0.317 (0.1374)
σ_w	0.01435	8935.8
R^2	0.4568	0.2907

Table 9. Parameter estimates and comparison of SAR(1) model for the series examined and goodness of fit index R^2; in parenthesis the standard deviation of the estimates

If the estimates are analyzed in greater detail, in the Figures 33a,b,c it may be noted that the parameters in question are statistically identical. Then the model reported in (48) was applied, only to three series of data obtained along the transect. The series concerns, in particular, values of soil water content θ and tension h obtained 48 hours from the beginning of the drainage. Furthermore the analysis will be extended to a section of the soil moisture retention curve θ(h) constructed for h=100 cm, subsequently indicated as θ_{-100}. More significantly, the essential characters assumed in the space from the distribution of the parameters in question may be deduced from the transects of Figure 33, which report the relative values in the 50 observation points.

To identify the ARMA models to be adapted to the above three series, we estimated the autocorrelation (ACF) and partial autocorrelation (PACF) function. As transpires from Figures 34a,b,c,d, the three series can be well represented by an ARMA (1,1) model.

Anyway analysis of ACF residuals (Figure 34d) shows clearly that no structure whatever is present in the series of noises, which is further confirmation of the good fit of the model used to represent the examined parameters.

Parameter estimates, obtained with the least squares method, of the ARMA(1,1) model adapted to the above series and the goodness index fit R^2 (mean square errors in brackets) are reported in table 10. Clearly, all three series show a strong inertia component which confirms the presence of the spatial structure ascribable to an AR(1), accompanied by marked fortuitousness as results from the low value of R^2.

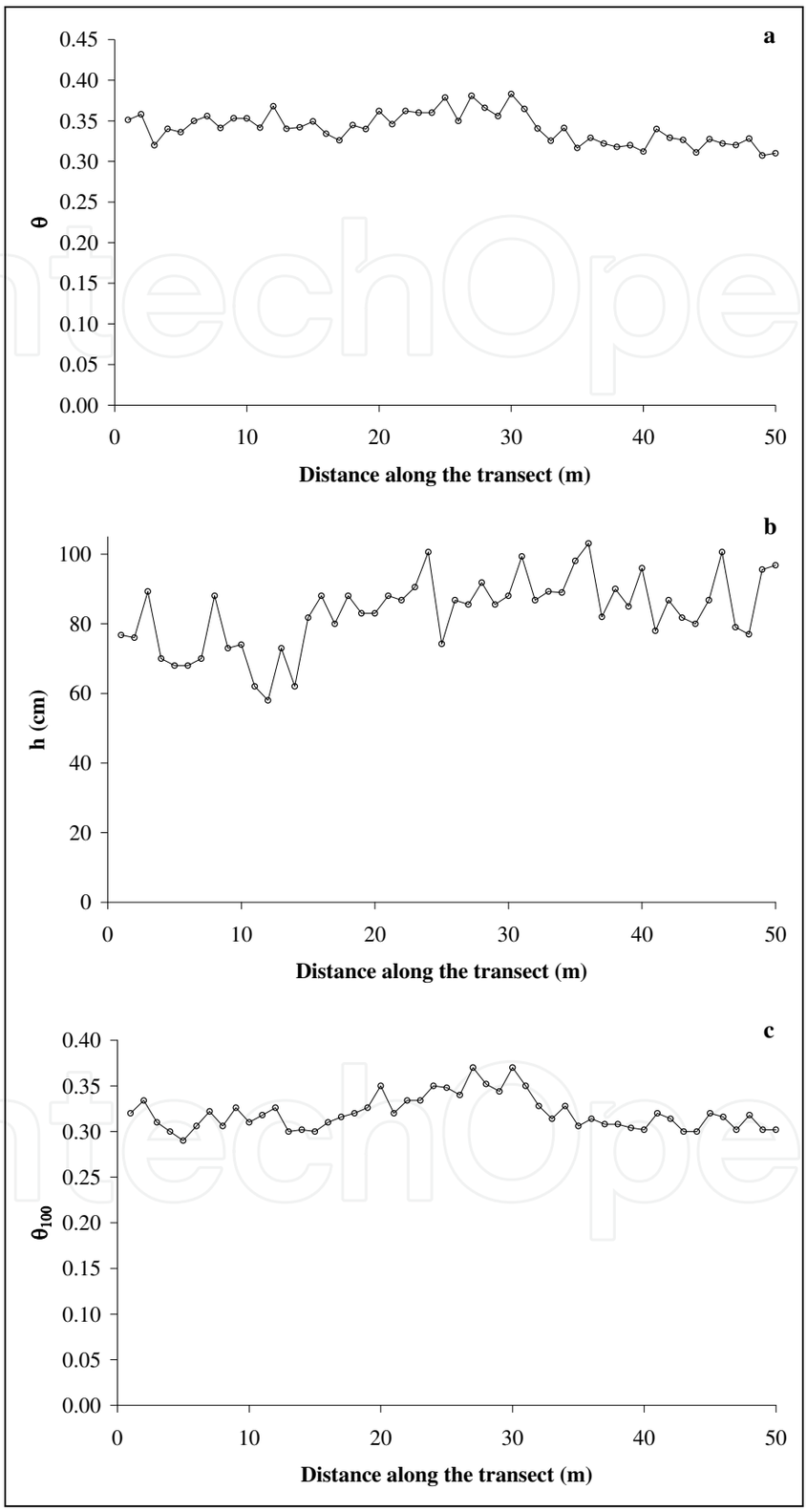

Fig. 33. Values of a. θ, b. h, c. θ_{100} along the transect

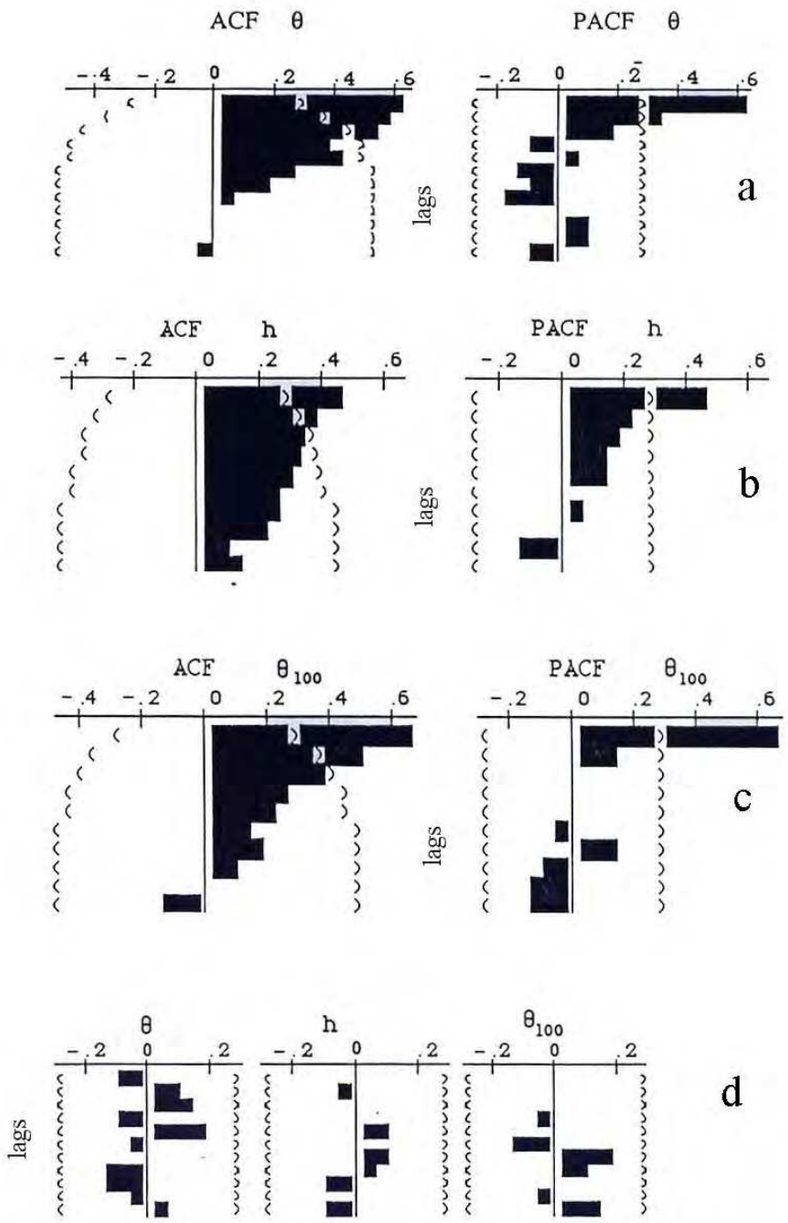

Fig. 34. Estimated ACF and PACF for a. θ, b. h, c. θ_{100} and d. noise in the model 1

	ϕ	α	$\hat{\sigma}_I$	R^2
θ_3	0.94 (0.075)	0.51 (0.12)	0.0136	0.501
h_3	0.91 (0.07)	0.63 (0.14)	8.729	0.300
θ_{100}	0.77 (0.10)	0.21 (0.10)	0.0110	0.392

Table 10. Parameter estimates of the ARMA(1,1) model, for θ_3, h_3, θ_{-100} and goodness of fit R^2. In parenthesis the standard deviations of the estimated parameters.

The estimated model was then used to obtain optimal predictions along the transect. Figure 35a, b reports the observed data, a signal estimate and the relative noise for series θ_3 and h_3. The graphs for the other series were similar, with analogous signal in the general pattern, not reported here for the sake of brevity, confirming that the spatial structure of soil hydraulic parameters is a characteristic of the porous medium in question.

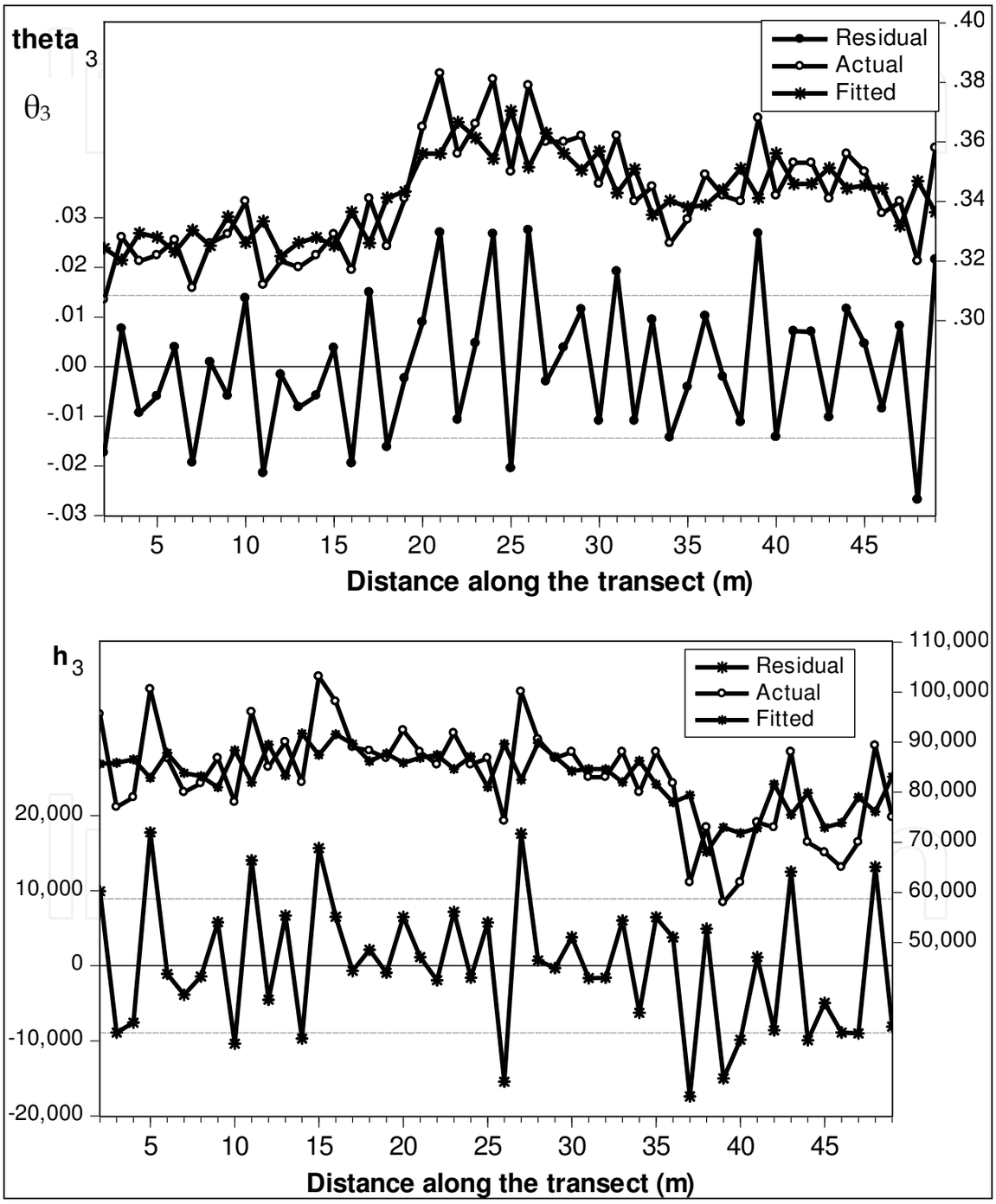

Fig. 35. Observed data, signal estimate and the relative noise for series a. θ_3 and b. h_3.

5. Conclusions

A determination of the hydraulic properties of soil is seen to be indispensable if we wish to approach the study of water movement in quantitative terms, using mathematical models. The practical possibilities of extensive application of such models implies the development of measuring techniques which render the determination of the laws θ(h) and K(θ) less problematic.

These proposed methods allow us readily to obtain functions θ(h) and K(θ), by submitting the samples, in the laboratory and in the open field, to a process of evaporation and internal drainage, respectively, and requires only the measurement of the mean water content and of the potentials at different depths along the soil sample or profile.

It was verified that the retention and conductivity curves thus determined and described, using analytic equations, can be used in simulation models with an acceptable degree of accuracy. Moreover, it can be observed that the duration of the tests was not excessive: this makes acceptable the labour intensiveness of characterization imposed on statistical evaluations of the variability of individual hydraulic parameters.

Therefore, from this proven association of accuracy and speed in the experimental work of characterization, we are convinced that the adopted methodologies can be considered adequate to the demands of modern study at an operative level of problems connected with water movement and of solutes in unsaturated media.

6. Appendix A

6.1 Hydraulic conductivity function

Hydraulic conductivity (K) is one of the most complex and important of the properties of vadose zone in hydro-physics and of aquifers in hydrogeology as the values found in nature:

- range of many orders of magnitude (the distribution is often considered to be lognormal);
- vary a large amount through space (sometimes considered to be randomly spatially distributed or stochastic in nature);
- are directional (in general K is a symmetric second-rank tensor; e.g.; vertical K values can be several orders of magnitude smaller than horizontal K values;
- are scale dependent;
- must be determined through field test, laboratory column flow test or inverse computer simulation;
- are very dependent in a non-linear way on the water content which makes solving the unsaturated flow equation difficult.

Some typical K(θ) curves for sandy and loamy soils are shown in Figure 1A. Note that at saturation the sandy soil has higher conductivity because of the larger water-filled pore spaces. These large pores drain at low suction, however, causing a considerable decrease in conductivity. The loamy soil, having smaller (on average) pores, retains a greater number of water-filled pores and thus has higher conductivity than the sandy soil at these potentials.

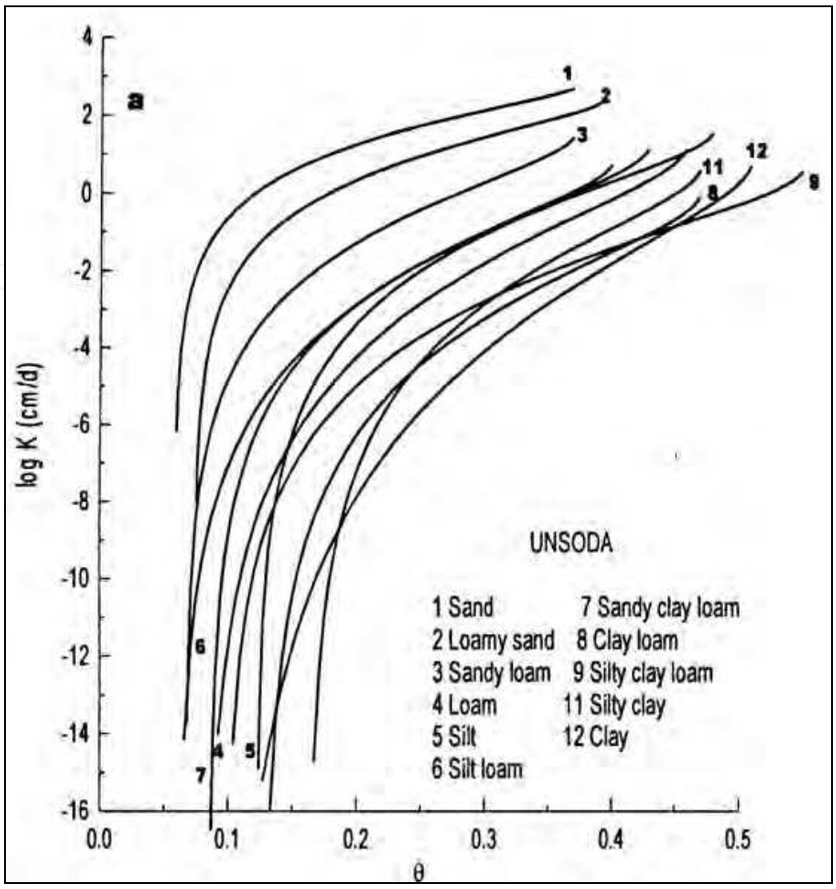

Fig. 1A. Typical unsaturated hydraulic conductivity curves for soils of different texture from UNSODA database. Source: Leij et al. (1996)

6.2 Parametric models for soil unsaturated hydraulic conductivity

In the past, many different functional relations have been proposed in the literature based on various combinations of the dependent variables θ, h and K, and a certain number of fitting parameters (Brooks and Corey, 1964; van Genuchten, 1980). Independent of the correct physical meaning of the fitting parameters, their values are submitted to constraints imposed by the use of the transfer equations such as the Fokker Planck and/or Richards equation. The most frequently used in the literature are the following water retention and hydraulic conductivity expressions:

Soil water characteristic functions

The Brooks and Corey (1964) equation:

$$\begin{aligned} \frac{\theta-\theta_r}{\theta_s-\theta_r} &= \left(\frac{h_{bc}}{h}\right)^{\lambda} && h \le h_{bc} \\ \theta &= \theta_s && h_{bc} \le h \le 0 \end{aligned} \tag{1A}$$

and the van Genuchten (1980) soil water characteristic equation:

$$\frac{\theta-\theta_r}{\theta_s-\theta_r}=\left[1+\left(\frac{h}{h_g}\right)^n\right]^m \tag{2A}$$

where the water pressure head (h) is usually taken as negative and expressed in cm of water; h_{bc} is the Brooks and Corey pressure scale parameter, h_g is the van Genuchten pressure scale parameter, and λ, m, and n are water retention shape parameters. The water retention shape parameters m and n are assumed to be linked by

$$m=1-\frac{k_m}{n} \quad n\geq k_m \tag{3A}$$

where k_m is an integer value initially introduced by van Genuchten (1980) to calculate closed-form analytical expressions for the hydraulic conductivity function when substituted in the predictive conductivity models of Burdine (1953) or Mualem (1976). For the Mualem theory, parameter k_m takes the value k_m =1, and for the Burdine theory k_m=2. For high pressure head values, the van Genuchten water retention equation behaves like the Brooks and Corey equation with $\lambda=mn$. However, it should be noted that this identity is only confirmed for soils with shape parameter values m <0.1 (for the case where the Burdine condition is used: k_m=2);

Hydraulic conductivity functions

The Brooks and Corey (1964) equation:

$$\frac{K}{K_s}=\left[\frac{\theta-\theta_r}{\theta_s-\theta_r}\right]^\eta \tag{4A}$$

and the van Genuchten-Mualem (1980) hydraulic conductivity equation:

$$\frac{K}{K_s}=\left[\frac{\theta-\theta_r}{\theta_s-\theta_r}\right]^{1/2}\left[1-\left\{1-\left(\frac{\theta-\theta_r}{\theta_s-\theta_r}\right)^{1/m}\right\}^m\right]^2 \tag{5A}$$

where η is a conductivity shape parameter.

Through an extensive study, Fuentes et al. (1992) concluded that only the combination of the van Genuchten water retention equation (equation 2A), h(θ), based on the Burdine theory (m=1-2/n) together with the Brooks and Corey conductivity equation (Equation 5A) stays valid for all different types of soil encountered in practice without becoming inconsistent with the general water transfer theory. This is due to the rather limiting constraint which exists for shape parameter m when using the Mualem theory : 0.15 ≤m≤1 Even though the residual water content (θ_r) has a well-defined physical meaning, the parameter θ_r, which enters in equations (1A) to (5A) is somewhat of a misnomer because it usually behaves as a pure fitting parameter without any physical meaning. For practical purposes, it can easily be set equal to zero (Kool et al., 1987).

The scale parameter K_s is strongly related to soil structure. Among the different soil hydraulic characteristic parameters the saturated hydraulic conductivity is the parameter which is the most influenced by effects such as macropores, stones, fissures, cracks, and other irregularities formed for various biological and mechanical reasons. Hence, it is the parameter which is the most difficult to predict. The models proposed in the literature either give estimations of the capillary conductivity value or are based on site and soil specific databases. The results should therefore be considered with caution when applied to field studies.

Mishra and Parker (1990) used the Mualem model (1976) with the van Genuchten water retention function (equation 2A) to obtain a closed-form expression of the saturated hydraulic conductivity:

$$K_s = c_1 \frac{\left[\theta_s - \theta_r\right]^{2.5}}{h_g^2} \tag{6A}$$

where c_1 is a constant including the effects of fluid characteristics and the porous media geometric factor; it has a value of 108 cm^3/s when K_s is expressed in cm/s; h_g is the van Genuchten (1980) pressure scale parameter. The authors derived a similar predictive equation by the use of the Brooks and Corey (1964) water retention equation (equation 1A):

$$K_s = c_1 \frac{\left[\theta_s - \theta_r\right]^{2.5}}{h_{bc}^2} \left[\frac{\lambda}{1+\lambda}\right]^2 \tag{7A}$$

where λ and h_{bc} are the Brooks and Corey (1964) shape and scale parameters, respectively. Ahuja et al. (1985) used the general Kozeny-Carman approach to determine the saturated hydraulic conductivity from the effective porosity (ε-θ_r):

$$Ks = c_2 \left[\varepsilon - \theta_r\right]^{c_3} \tag{8A}$$

where c_2 is equal to 1058 cm/h when K_s is expressed in cm/h; and c_3 takes a value of 4 or 5.

Estimation of van Genuchten and Brooks and Corey parameters from experimental data requires sufficient data points to characterize the shape of the curves, and a program to perform non-linear regression. In particular, computer programs for estimation of specific parametric models are also available, e.g., the RETC code (van Genuchten at al, 1991).

7. References

Ahuja L.R., B.B. Barnes, D.K. Cassel, R.R. Bruce, D.L. Nofziger (1988), Effect of assumed unit gradient during drainage on the determination of unsaturated hydraulic conductivity and infiltration parameters, *Soil Sci*., 145, 235-243.

Ahuja, L. R., Naney, J. W., and Williams, R. D. (1985), Estimating soil water characteristics from simpler properties or limited data. *Soil Sci. Soc. Am. J.* 49: 1100-1105.

Amoozegar-fard D., W.W. Warrick, Field measurements of saturated hydraulic conductivity (1986), In: a. Klute ed., methods of soil analysis, part 1: physical and mineralogical methods, monograph series 9. *Am. Soc. Agron*., Medison; WI

Anderson S.H., D.K. Cassel (1986), Statistical and autoregressive analysis of soil properties of Portsmouth sandy loam, *Soil Sci. Soc. Am. J.*, 50, 1096-1104.

Ankeny M.D., M. Ahmed, T.C. Kaspar, R. Horton (1991), Simple field method for determining hydraulic conductivity, *Soil Sci. Soc. Am. J.*, 55, 467-470.

Basile A., Coppola A., De Mascellis R., Randazzo L. (2006), A hysteresis based scaling approach to deduce field hydraulic behaviour from core scale measurements. *Vadose Zone Journal*, 5:1005–1016 (2006), doi:10.2136/vzj2005.0128

Basile, A., G. Ciollaro, and A. Coppola, 2003. Hysteresis in soil water characteristics as a key to interpreting comparisons of laboratory and field measured hydraulic properties, *Water Resour. Res.*, 39(12), 1355, doi:10.1029/2003WR002432.

Bear J. (1979), Hydraulics and groundwater, McGraw Hill, N.Y.

Beckett P.H.T. and R. Webster (1971). Soil variability: A review, *Soil and Fertilizers*, 34:1-15.

Boels D., J.B.H.M. Van Gils, G.J. Veerman , K.E. Wit (1978), Theory and system of automatic determination of soil moisture characteristics and unsaturated hydraulic conductivities, Soil Sci., 126, 191-199.

Booltink, H.W.G., J. Bouma, D. Gimenez (1991), Suction crust infiltrometer for measuring hydraulic conductivity of unsaturated soil near saturation, *Soil Sci. Soc. Am. J.*, 55, 566-568.

Bouma J. (1983), Use of soil survey data to select measurement techniques for hydraulic conductivity, Agric. Water Managem., 3, 235-250.

Bouma J., L.W. Dekker (1978), A case study on infiltration into dry clay soil, I. Morphological observations, *Geoderma*, 20, 27-40.

Bouma, J. (1982), Measuring hydraulic conductivity soil horizons with continuous macropores, *Soil Sci. Soc. Am. J.*, 46, 438-441.

Box, G.E.P., G.M Jenkins (1970), Time series analysis, forecasting and control, *Holden day*, San Francisco.

Bresler E., H. Bielorai, A. Laufer (1979), Field test of solution models in a heterogeneous irrigated cropped soil, *Water Resour. Res.* 15, 645-652.

Brooks, R. H. and Corey, C. T. (1964), Hydraulic properties of porous media. Hydrol. Paper 3. Colorado State University, Fort Collins.

Burdine, N. T. (1953), Relative permeability calculations from pore size distribution data. Petr. Trans.. Am. Inst. Mining Metall. Eng. 198: 71-77.

Burgess T.M., R. Webster (1980a), Optimal interpolation and isarithmic mapping of soil properties, I. The semi-variogram, and punctual kriging, *J. Soil Sci.*, 31, 315-331.

Carlos M.O., J.W Hopmans, M. Alvaro, L.H Bossai, D. Wildenschild (2002), Soil water retention measurement using a combined tensiometer-coiled time domain reflectometry probe, *Soil Sci. Soc. Am. J.*, 66, 1752-1759.

Cassel D.K., O. Wendroth, D.R. Nielsen (2000), Assessing spatial variability in an agricultural experiment station field: opportunities arising from spatial dependence, *Agron. J.*, 92, 706-714.

Chen C., R.J. Wagenet (l991), Simulation of water and chemicals in macropores soils, 1. Representation of the equivalent macropore influence and its effect on soil-water flow, *J. Hydrol.*, 130, 105-126.

Chong S.K., R.E. Green, L.R. Ahuja (1981), Simple in situ determination of hydraulic conductivity by power function descriptions of drainage, *Water Resour. Res.*, 17, 1109-1114.

Ciollaro G., V. Comegna, C. Ruggiero (1987), Confronto tra metodi di campo e di laboratorio per lo studio delle caratteristiche idrauliche del suolo, Hydraulic Agriculture Insitute, University of Naples.

Comegna V., Vitale C. (1993), Space-time analysis of water status on a volcanic Vesuvian soil. Geoderma 60:135-158.

Coppola A. (2000), Unimodal and bimodal descriptions of hydraulic properties for aggregated soils, *Soil Sci. Soc. Am. J.*, 64, 1252,1262.

Coppola A., A. Comegna, G. Dragonetti, M. Dyck, A. Basile, N. Lamaddalena, M. Kassab, V. Comegna (2011), Solute transport scales in an unsaturated stony soil, *Advan. Water resour.*, 34, 747-759.

Coppola, A., Basile A., Comegna A., Lamaddalena N. (2009), Monte Carlo analysis of field water flow comparing uni- and bimodal effective hydraulic parameters for structured soil, *Journal of Contaminant Hydrology*, doi:10.1016/j.jconhyd.2008.09.007.

Coppola, A., Randazzo, L. (2006). A MathLab code for the transport of water and solutes in unsaturated soils with vegetation. Tech. Rep. Soil and Contaminant Hydrology Laboratory, Dept. DITEC University of Basilicata.

Dane J.H. (1980), Comparison of field and laboratory determined hydraulic conductivity values, *Soil Sci. Soc.Am. J.*, 44: 228-231.

David G., Geostatistical ore reserve estimation (1977), *Elsevier*, N.Y..

Day, P.R., Methods of soil analysis. Part 1. Agronomy (1965). C.A. Black Amer. Soc. of Agron., Madison, Wis. 9, 545-556.

Elrick, D.E., Scandrett, JH., E.E. Miller (1959), Tests of capillary flow scaling, *Soil Sci. Soc. Am. Proc*. 23, 329-332.

Evett, S.R., Peters F. H., Jones S. R., and Unger P. W., 1999. Soil hydraulic conductivity and retention curves from tension infiltrometer and laboratory data. Proc. Int. Workshop Characterization and Measurement of the Hydraulic Properties of Unsaturated Porous Media --University of California, pp 541-551. van Genuchten M. Th. and Leij F. J. Edt.

Frenkel H., J.O. Goertzen, J.D.R. Hoades (1978), Effects on clay type and content , exchangeable sodium percentage, and electrolyte concentration on clay dispersion and soil hydraulic conductivity, *Soil Sci. Soc. Am. J.*, 42, 32-39.

Fuentes, C., Haverkamp, R., and Parlange, J. Y. (1992), Parameter constraints on closed form soil water relationships. *J. Hydrol.* 134: 117-142.

Gajem, Y., A.W. Warrick, D.E. Myers (1981). Spatial dependance of physical properties of typic torrifluvent soil, Soil Sci. Soc. Am. J., 45, 709-715.

Gardner W.R. (1958), Some steady-state solutions of the unsaturated moisture flow equation with applications to evaporation from a water table, *Soil Sci*., 85, 228-232.

Gerke, H.H., M.T. van Genuchten (1993), A dual-porosity model for simulating the preferential movement of water and solutes in structured porous media, *Water Resour. Res*., 29, 305-319.

Heuvelink G.B.M., R. Webster (2001), Modeling soil variation: past, present and future, Geoderma, 100, 269-301.

Hillel, D., Environmental Soil Physics, (1998), *Academic press*, N.Y..

Hopmans J.W., J.M.H. Hendrickx, Selker J.S, (1999), Emerging measurement techniques for vadose zone characterizations. In vadose zone hydrology, Parlange and Hopmans (eds), *Oxford University Press*.

Jarvis N.J.P., P.E. Janson, P.E. Dik, I. Messing (1991), Modeling water and solute transport in macroporous soil, 1. Model description and sensivity analysis, *J. Soil Sci*, 42, 59-70.

Jensen, M.E. (1980), Design and operation of larm irrigation system, *American Society of Agricultural Engeeniers*, St. Joseph

Jones A.J., R.J. Wagenet, (1984), In situ estimation of hydraulic conductivity using simplified methods, *Water Resour. Res.*, 20, 1620-1626.

Journel A.G., C.H.J. Huijbregts (1978), Mining Geostatistic, *Accademic Press*, London.

Jury W., W.R. Gardner and W. H. Gardner (1991). Soil Physics. John Wiley and Sons Inc., ISBN 0-471-83108-5.

Kalman R.E., A new approach to linear filtering and predictions problems (1960), *Transactions of Asma, D. Jour. of Basic Enginering*, 82, 35-45.

Klute A. (ed.) (1986), Methods of soil analysis. Part 1. 2nd ed. *Agron. Monogr. 9 ASA and SSSA*, Madison, WI.

Klute A., G.E. Wilkinson (1958), Some tests of similar media concept of capillary flow: I. Reduced capillary conductivity and moisture characteristic data, *Soil Sci. Soc. Am. Proc.* 22, 278-281.

Kool, J. B., Parker, J. C., and van Genuchten, M. Th. (1987), Parameter estimation for unsaturated flow and transport models — A review. *J. Hydrol*. 91: 255-293.

Kutilek, M., and D. R. Nielsen (1994), Soil Hydrology, 370 pp., Catena, Cremlingen-Destedt, Germany.

Lax P.D. (1972), The formation and decay of shock waves. *Am. Math. Month.*, 79, 227-241, 1972.

Leij, F. J., Alves, W. J., van Genuchten, M. Th., and Williams, J. R. (1996), The UNSODA — Unsaturated Soil Hydraulic Database — User's Manual Version 1.0. Report EPA/600/R-96/095. National Risk Management Research Laboratory, Office of Research Development, U.S. Environmental Protection Agency, Cincinnati, Ohio: 1-103.

Libardi P.L., K. Reichardt, D.R. Nielsen, J.W. Bigger (1980), Simple field methods for estimating soil hydraulic conductivity, *Soil Sci. Soc. Am. J.*, 44, 3-7.

Matheron G., The theory of regionalized variables and its application (1971), *Ecole des mines de paris*. Fontainbleau, France.

Messing I., N.J. Jarvis (1993), Temporal variation in the hydraulic conductivity of a tilled clay soil as a measured by tension infiltrometers, *J. Soil Sci*., 44, 11-24.

Miller E.E.., R.D. Miller (1955a), Theory of capillary flow: I. Practical implications, *Soil Sci. Soc. Am. Proc.*, 19, 267-271.

Miller, E.E., R.D. Miller (1955b), Theory of capillary flow: II. Experimental information, *Soil Sci. Soc. Am. Proc.* 19, 271-275.

Mishra, S. J. and Parker, J. C. (1990), On the relation between saturated hydraulic conductivity and capillary retention characteristics. *Ground Water*. 28: 775-777.

Morkoc F., J.W. Biggar, D.R. Nielsen, D.E. Rolston (1985), Analysis of soil water content and temperature using state-space approach, *Soil sci. Soc. Am. J.*, 49, 798-803.

Mualem Y., G. Dagan (1975), A dependent demain model of capillary histeresis, *Water Res. Res*., 11, 452-460.

Mualem, Y. (1974), A conceptual model of hysteresis. *Water Resour. Res*. 10: 514-520.

Nielsen D.R., J.W. Biggar K.T. Erh (1993), Spatial variability of field-measured soil-water properties. Hilgardia. 42:215-259.

Nielsen D.R., O. Wendroth (2003), Spatial and temporal statistics. *Series: Advances in Geoecology*, Catena.

Peck A.J., R.J. Luxmoore, J.L. Stolzy (1977), Effects of spatial variability of soil hydraulic properties in water budget modeling. *Water Resour. Res.*, 13, 348-354.

Perroux K.M., I. White (1988), Designs for disc permeameters, *Soil Sci. Soc. Am. J.*, 52, 1205-1214.

Philip J.R. (1966), A linearization change for the study of infiltration, In water in the unsaturated zone, *Unesco symp.*, 471-478.

Philip J.R. (1969), Theory of infiltration, *Advances in hydroscience*, 5, 215-296.

Philip J.R. (1985), Reply to comments on `steady infiltration from spherical cavities", *Soil Sci. Soc. Am. J.*, 49, 788-789.

Philip J.R. (1986) Linearized unsteady multidimensional infiltration, *Water Resour. Res.*, 22, 1717-1727.

Poulsen T.G, P. Moldrup, O. Wendroth, D.R Nielsen (2003), Estimating Saturated hydraulic conductivity and air permeability from soil physical properties using state-space analysis, *Soil Science* 168, 311-320.

Raats P.A.C. (1976), Analytical solutions of a simplified flow equation, *Trans. Am. Soc. Agric. Eng.*, 19, 683-689.

Rao P.S.C., R.E. Jessup, A.C. Hornsby D.K. Cassel, W.A. Pollans (1983), Scaling soil microhydrologic properties of lakeland and konawa soils using similar media concepts, *Agric. Water Manage.*, 6, 277-290.

Regalado C.M., R. Munoz Carpena, A.R.M. Socorro, J.M. Hernadez Moreno (2003), Time Domain Reflectometry Models as tool to understand the electric response of volcanic soils, *Geoderma*, 117, 313-330.

Russo, D. and Bresler, E. (1980), Scaling soil hydraulic properties of a heterogeneous field. *Soil sci. Soc. Am. J.* 44:681-684.

Schuh W.M., J.W. Bauder, S.C. Gupta (1984), Evaluation of simplified methods for determining unsaturated hydraulic conductivity of layered soil, *Soil Sci. Soc. Am. J.*, 48, 730-736.

Scotter D.R., B.E. Clothier, E.R. Harper (1982), Measuring saturated hydraulic conductivity and sorptivity using twin rings.aust, *J. Soil res.* , 20, 295-304.

Sharma M.L., R.J. Luxmoore (1979), Soil spatial variability and its consequences on simulated water balance, *Water Resour. Res.*, 15:1567-1573.

Shumway R. H., D. S. Stoffer (2000), Time series analysis and its applications, *Springer Verlag*, N.Y..

Simmons C.S., D.R. Nielsen, J.W. Biggar (1979), Scaling of field-measured soil-water properties, *Hilgardia*. 47, 77-173.

Sisson J.B., A.H. Ferguson, M.Th. Van Genuchten (1980), Simple method for predicting drainage from field plot, *Soil Sci. Soc. Am. J.*, 44, 1147-1152.

Sisson J.B., M.Th. van Genuchten (1991), An improved analysis of gravity drainage experiments for estimating the unsaturated soil hydraulic functions. *Water Resour. Res.*, 27, 569-575.

Smettem K.R.J., B.E. Clothier (1989), Measuring unsaturated sorptivity and hydraulicc conductivity using multiple disc permeameters., *J. Soil Sci.*, 40, 563-568.

Snedecor G.W., W.G. Cochran (1980), Statistical methods, 7th edition, *Iowa State Universiry Press*, Ames, Iowa.

Tamari, S., L. Bruckler, J. Halbertsma, and J. Chadoeuf (1993), A simple method for determining soil hydraulic properties in the laboratory, Soil Sci. Soc. Am. J., 57, 642– 651.

Tillotson P.M., D.R. Nielsen (1984), Scale factors in soil science, *Soil sci. Soc. Am. J.*, 48, 953-959.

Topp G.C., J.L. Davis, A.P. Annan (1980), Electromagnetic determination of soil water content: measurement in coaxial transmission lines, *Water Resour. Res.*, 16, 574-582.

Van Dam, J.C., Huygen, J., Wesseling, J.G., Feddes, R.A., Kabat, P., van Walsum, P.E.V., Groenendijk, P., van Diepen, C.A. (1997), SWAP version 2.0, Theory. Simulation of water flow, solute transport and plant growth in the Soil-Water-Atmosphere-Plant environment. Technical Document 45, DLO Winand Staring Centre, Report 71, Department Water Resources, Agricultural University, Wageningen.Ahuja L.A., J.W. Naney,D.R. Nielsen (1984), Scaling soil water properties and infiltration modelling, *Soil Sci. Soc. Am. J.*, 48, 970-973.

van Genuchten M.Th. (1980), A closed-form equation for predicting the hydraulic conductivity of unsaturated soils, *Soil Sci. Soc. Am. J.*, 44, 892-898.

van Genuchten M.Th.., D.R. Nielsen (1985), On describing and predicting the hydraulic properties of unsaturated soils, *Ann. Geophys*, 3, 615-628.

van Genuchten, M. Th., Leij, F. J., and Yates, S. R. (1991), The RETC code for quantifying the hydraulic functions of unsaturated soils, EPA/600/2-91/065, US Environmental Protection Agency, Ada, OK.

Vauclin M., G. Vachaud (1987), Caracterisation hydrodynamique des sols: analyse simplifie des essais de drainage interne, *Agronomie*, 7, 647-655.

Vauclin M., S.R. Viera, R. Bernard, J.L. Haffield (1982), Spatial variability of surface temperature along two transects of a bare soil, *Water Resour. Res*., 18, 1677-1686.

Vieira S.R., J.L. Hatfield, D.R. Nielsen, J.W. Biggar (1983), Geostatistical theory and applications to variability of some agronomical properties, *Hilgardia*, 51, 1-72.

Warner G.S., I.D. Moore, J.L. Nieber, R.L. Geise (1989), Characterization of macropores in soil by computer tomography, *Soil Sci. Soc. Am. J.*, 53, 653-660.

Warrick A.W. (1992), Models for disc infiltrometers, *Water Resour. Res*., 28, 1319-1327.

Warrick A.W., A. Amoozegar-fard (1979), Infiltration and drainage calculations using spatially scaled hydraulic properties, *Water Resour. Res*., 15, 1116-1120.

Warrick A.W., G.J. Mullen, D.R. Nielsen (1977b), Scaling field-measured soil hydraulic properties using a similar media concept, *Water Resour. Res*., 13, 355-362.

Watson K.K. (1966), An instantaneous profile method for determining the hydraulic conductivity of unsaturated porous materials, *Water Resour. Res*., 2, 709-715.

Watson K.W., R.J. Luxmoore (1986), Estimating macroporosity in a forest watershed by use of a tension infiltrometer, *Soil Sci. Soc. Am. J.* , 50, 578-582.

Webster R. (1977), Spectral analysis of gilgai soil, *Aust. J. Soil Res*, 15, 191-204.

Webster R., C.H.E. Cuanalo De La (1975), Soil transect correlogram of north oxford shire and their interpretation, *J. Soil. Sci.*, 26, 176-194.

Wendroth O., A.M. Al-Omran, C. Kirda, K. Reichardt, D.R. Nielsen (1992), State-space approach to spatial variability of crop yield, *Soil Sci. Soc. Am. J.* 56, 801-807.

Wendroth O., S. Koszinski, E. Pena-Yewtukhiv (2006), Spatial association between soil hydraulic properties, soil texture and geoelectric resistivity, *Vadose Zone J.*, 5, 341-355.

White I., M.J. Sully (1987), Macroscopic and microscopic capillary length and time scales from field infiltration, *Water Resour. Res.*, 23, 1514-1522.

Wind, G. P. (1968), Capillary conductivity data estimated by a simple method, in Water in the Unsaturated Zone, vol. 1, edited by P. E. Rijtema and H. Wassink, Int. Assoc. Sci. Hydrol. Publ., 82– 83, 181– 191.

Wooding R.A. (1968), Steady infiltration from a shallow circular pond, *Water Resour. Res.*, 4, 1514-1522.

Wu, L., W.A. Jury, A.C. Chang, R. R. Allmaras (1997), Time series analysis of field-measured water content of a sandy soil, *Soil Sci. Soc. Am. J.*, 61, 736-742.

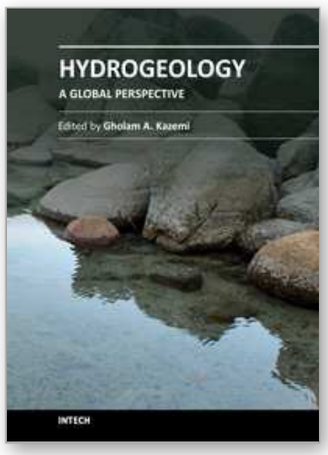

Hydrogeology - A Global Perspective
Edited by Dr. Gholam A. Kazemi

ISBN 978-953-51-0048-5
Hard cover, 222 pages
Publisher InTech
Published online 10, February, 2012
Published in print edition February, 2012

The field of groundwater hydrology and the discipline of hydrogeology have attracted a lot of attention during the past few decades. This is mainly because of the increasing need for high quality water, especially groundwater. This book, written by 15 scientists from 6 countries, clearly demonstrates the extensive range of issues that are dealt with in the field of hydrogeology. Karst hydrogeology and deposition processes, hydrogeochemistry, soil hydraulic properties as a factor affecting groundwater recharge processes, relevant conceptual models, and geophysical exploration for groundwater are all discussed in this book, giving the reader a global perspective on what hydrogeologists and co-scientists are currently working on to better manage groundwater resources. Graduate students, as well as practitioners, will find this book a useful resource and valuable guide.

InTech Europe
University Campus STeP Ri
Slavka Krautzeka 83/A
51000 Rijeka, Croatia
Phone: +385 (51) 770 447
Fax: +385 (51) 686 166
www.intechopen.com

InTech China
Unit 405, Office Block, Hotel Equatorial Shanghai
No.65, Yan An Road (West), Shanghai, 200040, China
中国上海市延安西路65号上海国际贵都大饭店办公楼405单元
Phone: +86-21-62489820
Fax: +86-21-62489821

IntechOpen